Delimiting the effects of lahars at Fuego volcano, Guatemala, during the next significant tropical storm

By

Mustafa Gokhan ALTINSOY

A thesis submitted to the University of Bristol in accordance with the requirements of the degree of MASTER OF SCIENCE in the Faculty of Earth Science.

Supervisors: Dr Matthew Watson

MSc Volcanology – School of Earth Sciences, September 2020

Abstract

Lahars are debris flows formed by the combination of volcanic material with water. They, can develop in large volumes and speeds, and cause loss of life and damage to property. Fuego volcano, Guatemala is a highly active volcano, where and lahars occur frequently. The occurrence of lahars in tropical conditions with high rainfall can increase their volume and destructiveness.

Modelling of lahars, determination of hazardous areas, and ready evacuation plans in case of possible danger will minimise loss of life and property. For this purpose, lahars were modelled at Fuego, and impact areas that may occur in a tropical storm were calculated. The focus was on the Ceniza Valley, due to significant nearby population centres, using two different hazard models, Laharz and LaharFlow. Potential hazard areas were identified by evaluating results of the two models, together with the advantages and disadvantages of both programs.

We found that for a lahar to occur in the Ceniza valley, there must be more than 10- mm of precipitation. Also, we determined that the Plataranes and Melina streams converge in the Ceniza valley, this potentially increases the lahar volume in the Ceniza valley. We have seen that lahars occurring of volumes larger than 10^6 m^3 will adversely affect the settlements of Las Palmas, Ingenio Pantaleon, Siquinala, Panimache, Morelia, Los Yucales, La Rochela and San Andres Osuna. We have presented our ideas on how evacuations might be undertaken and what could be done to reduce the risks.

Keywords: Modelling, ESRI ArcGIS, Spatial data, DEM, tropical storm, lahar, hazard mitigation, hazard assessment, Laharz, LaharFlow, Matlab

Dedication and Acknowledgements

First of all, I want to thank the Republic of Turkey Ministry of National Education and M.T.A. (General Directorate of Mineral Research and Exploration) for their financial support. Thank you to my advisor, Matthew Watson, who helped me with my studies. Thank you to my aunt and her family, who always supported me, and thank you also to my family who has always been with me.

Author's Declaration

"I declare that the work in this dissertation was carried out in accordance with the requirements of the University's Regulations and Code of Practice for Taught Programmes and that it has not been submitted for any other academic award. Except where indicated by specific reference in the text, this work is my own work. Work done in collaboration with, or with the assistance of others, is indicated as such. I have identified all material in this dissertation which is not my own work through appropriate referencing and acknowledgement. Where I have quoted or otherwise incorporated material, which is the work of others, I have included the source in the references. Any views expressed in the dissertation, other than referenced material, are those of the author."

Mustafa Gokhan ALTINSOY

06/09/2020

Table of Contents

Abstract I
Dedication and Acknowledgements II
Author's Declaration III
1. Introduction 1
1.1. Location (Fuego) 1
1.2. Organization and Goals 2
2. Background 4
2.1. Geological Structure 4
2.2. Previous Eruptions and Lahar Flows 7
2.3. Hydrology 11
3. Lahars 13
3.1. Rainfalls, Tropical Storms and Hurricanes 13
3.2. Lahar volumes used in the scenario-based study 15
4. Lahar Modelling in the Ceniza Barranca 16
4.1. Laharz 16
4.1.1. Lahar models in Laharz 19
4.2. LaharFlow 23
4.2.1. Lahar models in LaharFlow 27
4.3. Affected areas and the evaluation of data 31
5. Discussion 34
5.1. Uncertainties 40
5.2. Mitigation of risk 41
6. Conclusions 42
7. References 43
8. Appendices 49

1. Introduction

1.1. Location (Fuego)

Fuego volcano or Volcán de Fuego (14.473°N, 90.88°W; 3763 m asl) is one of the most active volcanoes in the world, located in the south of Guatemala (Martin and Rose, 1981; Global Volcanism Program, 2013) (Figure 1.1). The first written evidence for an eruption of Fuego appears in the letters of Pedro de Alvarado in 1524 (Kurtz, 1913). Since that date, more than 50 explosions have occurred at Volcanic Explosivity Index (VEI) two and above (Naismith et al., 2019). Low-density Strombolian eruptions (Patrick et al., 2007), lava fountains, and less frequently explosive eruptions occur at Fuego volcano (Escobar-Wolf, 2013; Rader et al., 2015).

As a result of a volcanic eruption, lahar flows occur as mass movements, resulting directly from a volcanic eruption and are called primary lahars. Primary lahars often develop in the range of 10^3 and 10^5 m^3 /s but can be between 10^7 and 10^9 m^3 /s during heavy rain, for example, a tropical storm. Secondary lahars, in contrast, are formed as a result of carrying pyroclastic material, from previous eruptions, together with rain (Cando-Jácome and Martínez-Graña, 2019). Even after an eruption, some volcanoes pose the danger of lahars. For example, as a result of the eruption of Mayon Volcano, in the Philippines in 1978, no lahar flow occurred. However, because of pyroclastic material accumulated near the volcano triggered by a typhoon in 1981, lahar flows subsequently occurred (Rodolfo, 1989).

Primary and secondary lahars can develop very quickly and pose a significant risk for settlements located near the volcano (Canuti et al., 2002). They cause loss of agricultural areas, damage to infrastructure, and loss of life and property (Rodolfo, 1989). Globally, seventeen per cent of deaths related to volcanic activity arise from lahar flows (Auker et al., 2013). For this reason, working on a scenario basis before the lahar flows that may occur, and informing policymakers, and local administrations about this issue will minimize these risks.

For this purpose, the Ceniza Valley, one of the seven drainage ravines at Fuego, has been studied. These drainage channels are locally known as barrancas, and they control the movement of lava flows, pyroclastic flows, and lahar flows (Figure 1.1).

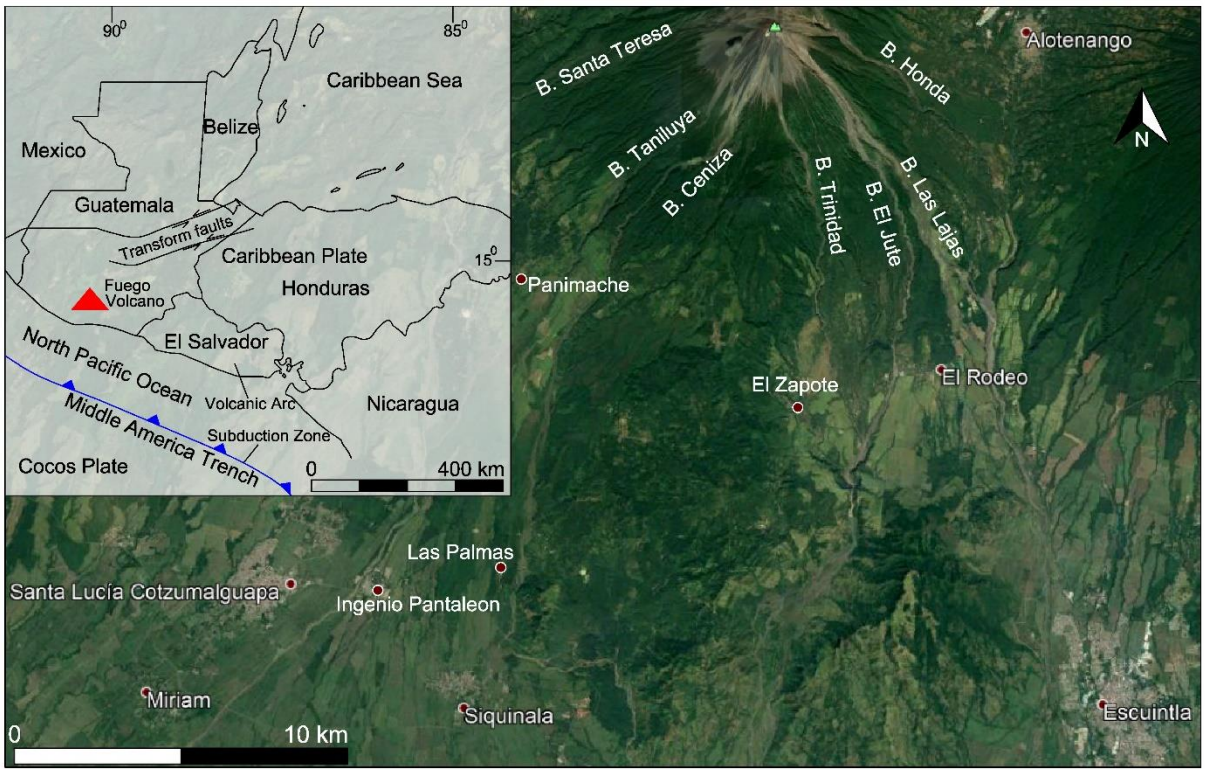

Figure 1.1. The location of the Fuego volcano in Central America and Guatemala, and Fuego's seven barrancas. Map Data: Google Earth Pro 7.3.3.7699, the inset is simplified from Duffield and others (1989).

1.2. Organization and Goals

The aims of this thesis are as follows:

- To examine and model lahar flows in Ceniza barranca, one of the seven drainage valleys around Fuego volcano, under tropical storm conditions.
- To identify the effects of the next lahar by examining historical lahar records and the geological features of Fuego.
- Comparing the results from a statistical model (Laharz) and a physical model (LaharFlow)
- To make recommendations for limiting these effects and minimising risks.

This thesis starts with the introduction and consists of six parts. The second section presents a background and a literature study of the previous eruptions of Fuego. The aim here is to determine the volumes that can affect the lahar streams that may occur later. The geology of the region, another important factor that may affect the movement of lahar flows, is examined,

and a geology map of the region is presented. After that, previous eruptions and the lahar activities that developed accordingly are examined. Then, the hydrogeology of the study area is investigated to determine the behaviour of the lahar flows that may occur.

In the third part of the thesis, precipitation, which is another factor affecting lahar flows, has been investigated. In order to make a comparison, the amount of rain falling on standard days (rainy and dry seasons) is taken and plotted. Then, storm and extreme rainfall conditions are evaluated, and possible flows of lahar are determined.

The fourth part involves numerical modelling. Two lahar models were used within the scope of this study. The first is the Laharz program, which is used in conjunction with Matlab software. First of all, information is given about the working principle of these programs. Thereafter, flow models digitised through these programs were collected in the ARGIS program. The second is the LaharFlow program. In this program, potential flow models are determined by initiating a physical model using the same input volumes as used in Laharz. Then, these data were evaluated at the end of this section. Settlements, agricultural lands, infrastructures and superstructures at risk of being affected have been identified near Fuego. The impact of a sudden flow on structures and people in this area has been evaluated, and recommendations are made in this regard.

In the fifth chapter, the models are compared. The advantages and disadvantages of both models and the output parameters are evaluated.

In the last part, all parameters and data obtained are evaluated. Accordingly, the obtained findings are shared.

2. Background

Volcanic mud- flows, commonly known as lahars, are volcanic hazards caused by the combination of materials produced by volcanic activities with water. Because of their rapid movements and destructive effects, they pose a high risk for people and settlements (Smith and Fritz, 1989, Vallance et al. 2015, Jones et al., 2017). For this reason, it is essential to determine the lahar flows that may occur, and the conditions that trigger the lahars.

Previous volcanic eruptions should be understood, and their effects must be investigated to determine the effects of the next large lahars. For this purpose, in the first part of this section, the geological structure is examined. The previous explosions and the destructive activities of the lahars that developed are examined in the second part. In the last part of this section, the hydrology of the Fuego and its surroundings are analysed. The catchment area is defined, and streams that can be activated in the lahar flow have been identified.

2.1. Geological Structure

Fuego volcano consists of basaltic and andesitic products. While the old rocks are more silicic, the rock units formed after the 1974 explosion are basalt rich in aluminium. (Chesner and Rose, 1984; Roggensack, 2001). In terms of the historical formation process, Fuego complex consists of Fuego and Meseta vents. As a result of the collapse of the Meseta vent, debris-avalanche units that have reached the Pacific coast have formed (GVP, 2013). Figure 2.1 shows the geological units of Fuego and its surroundings.

Rocks and erodible materials (alluvion, volcanic avalanches, and fluvial fans, as can be seen in Figure 2.1) carried by previous lahar activities pose a risk to people and settlements. Rock movements may cause deaths and severe injuries and may damage engineering structures in residential areas. As a result of erosion, lahar volume and destructiveness can increase significantly.

In mass movements, the distance travelled by the material depends on the angle of the slope and the momentum. Near the summit where the slope is approximately 40 degrees and above, the rocks can move up to a few kilometres. When the angle of the slope decreases to below ~30 to 35 degrees, or when the channels become narrow, the movement will slow down due to the momentum loss (Escobar-Wolf, 2013). Rock blocks, especially 2-3 meter blocks (Table 1), which may bounce from the channels, will damage agricultural lands and settlements. Rock blocks, especially blocks of two to three metres in diameter blocks (Table 1), which may bounce from the channels, will damage agricultural lands and settlements.

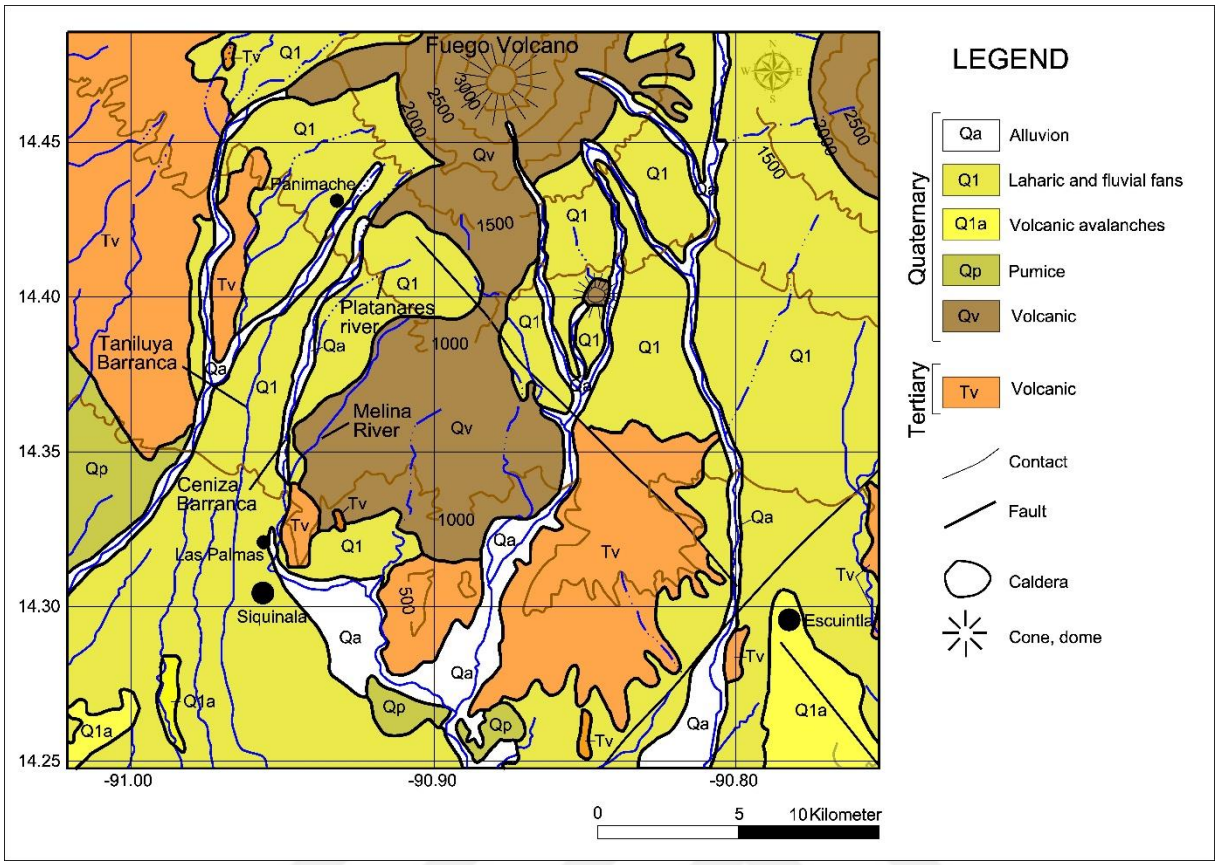

Figure 2.1. Geological map of Fuego volcano and its surroundings, adapted from Bonis, 1993

In the Ceniza barranca, the average slope of about 2.5 kilometres from the volcanic vent is above 30 degrees. Erosion, rock falls, and material transportation frequently occur in this area. The average slope from here to the Siquinala settlement will be slightly above about five degrees, and in this section, there will be transportation and sedimentation.

Average and extreme rains cause erosion of the previously accumulated volcanic and pyroclastic deposits. The volume of pyroclastic deposit in Las Lajas barranca is between 20 and 30 million m^3 (Naismith et al., 2019). This number can be compared with the pyroclastic volumes produced by paroxysms between 1999 and 2018. The eruption on 21 May 1999 produced 0.0255 km^3 of pyroclastic material. The eruption on 13 September 2012 produced 0.0269 km^3 pyroclastic flow material. Also, paroxysms occurring since 2015 indicate two critical risks, namely that (1) pyroclastic flows can be produced in more than one barranca, so the risk increases in more than one area at the same time, and (2) areas that are considered not to be at risk may also be at risk (Naismith et al., 2019).

The Ceniza barranca is seen in Figure 2.2. In addition to the occurrence of erosion, rockfalls and transport in this area, blocks separated from bedrock will stop at the point where they lose their momentum, and they will pose a risk to the settlements and people in the next lahar stream.

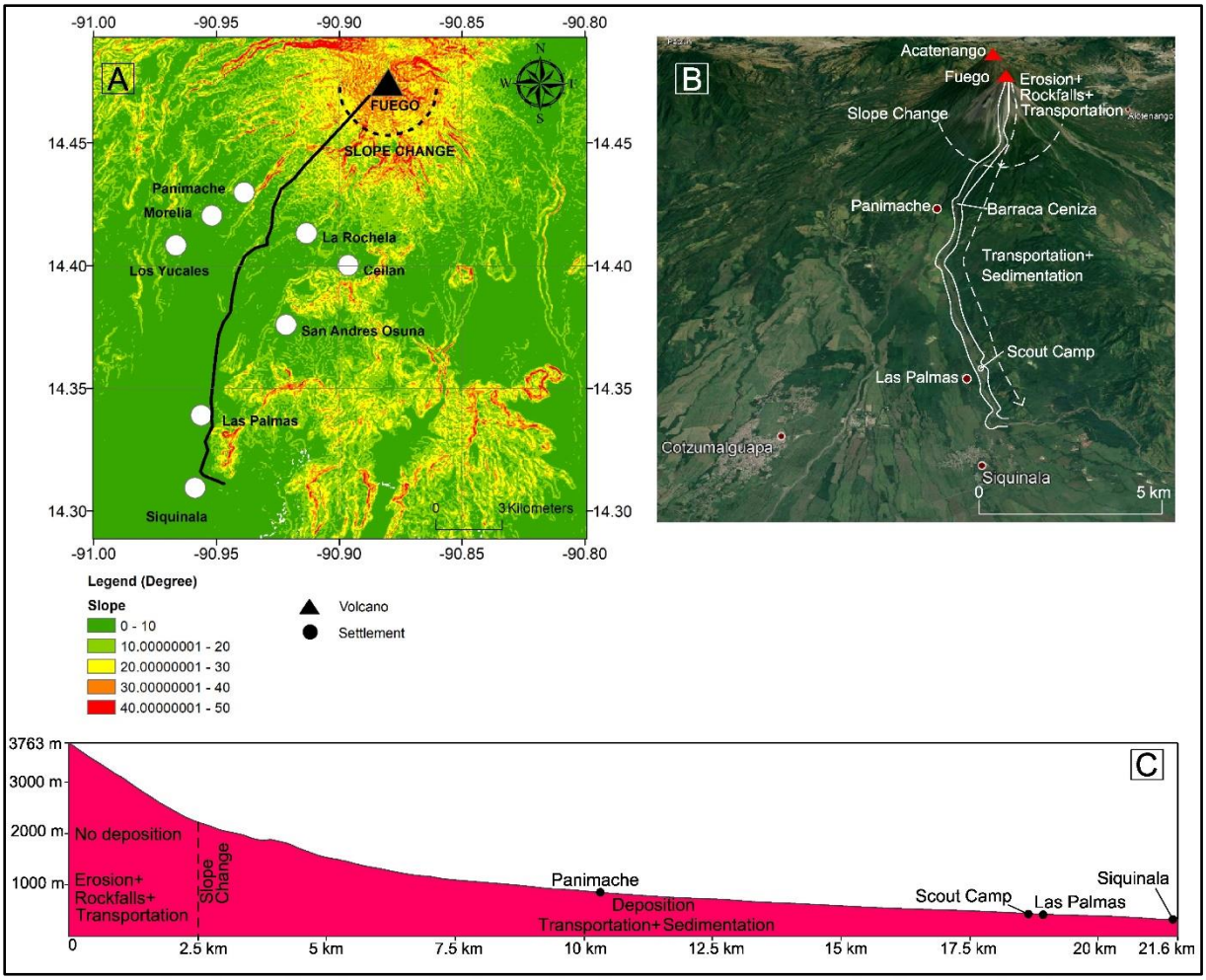

Figure 2.2. A. Presents a slope index map of the Fuego volcano. The colours show the values of the slope intervals (prepared in ArcGIS using the digital elevation model). B. Transport and deposition of materials in a lahar stream that may occur in the Ceniza barranca. C. Cross-section of the Ceniza barranca. Map Data: Google Earth Pro 7.3.3.7699

The slope angle is approximately five degrees from the point where the slope changes to the settlement of Siquinala. In this area transportation and sedimentation occur during extreme rainfall, and in sections where the depth of the channel decreases, the rapidly flowing lahars expand laterally and pose a risk for the surrounding settlements. The lahars that have occurred since 2015 have covered immense distances. For example, a lahar destroyed a scout camp in August 2017 (Finca Scout, coordinates: 14.34 N, 90.95 W), and it destroyed a bridge over the Ceniza River, 20 km below Fuego, very close to the scout camp. Therefore, Las Palmas, which is located close to the scout camp, will be at risk as a result of a large lahar that may develop, as evacuation options are very limited.

Since it is challenging to estimate the erosion that can occur in the channel, vertical dimensions should be determined at several points. In a study conducted on 29 June 2003, the average

storage was found to be 17 meters on average. However, this depth can be different in each channel. The stored material ranges from 2- m to 35- m in depth, and values in this range can be used to estimate the deposit volume, but best estimates can be obtained by field study and observations (Escobar-Wolf, 2013).

2.2. Previous Eruptions and Lahar Flows

Fuego volcano is located at the junction of the Caribbean, Cocos and North American plates (Figure 1.1). The compression and translational forces occurring in these plates control the behaviour of the Central American volcanic arc (Álvarez-Gómez et al., 2008; and Authemayou et al., 2011).

Fuego's volcanic activity period is examined in two parts. The first part focuses on the activity period between 1524 and 1999. The behaviour of the volcano during this period is examined in three ways: (1) lava flows, (2) low-density Strombolian eruptions, and (3) larger eruptions with higher energy (ash-rich eruptions), a cycle that has been repeated throughout the activity period (Patrick et al., 2007; Naismith et al., 2019). The second part focuses on the new eruption period between 1999 and 2018. During this period, permanent Strombolian eruptions prevail, and the process is punctuated by lava flows or greater energy eruptions (Naismith et al., 2019).

The recent period of activity has been studied by INSIVUMEH (The National Institute for Seismology, Vulcanology, Meteorology and Hydrology), a scientific agency in Guatemala. The Fuego Observatory was set up as a result of the reinitiation of volcanic activity in 1999. In general, during effusive background activity, the lavas reach up to 300 meters on average, the lavas in medium-level activism, for example before a larger eruption, reach up to 1 km (Escobar- Wolf, 2013). Also, Fuego volcano produces thousands of eruptions identified as Strombolian within a few hours during lava effusion (Blackburn, 1976). In these eruptions, the eruption columns rise 50-500 meters from the summit. Larger explosions occur less frequently compared to lava effusions. As a result of these explosions, a large amount of pyroclastic material, ballistics, and tephra occur (Lyons et al., 2010). The activity of the Fuego volcano has significantly affected the people living near the volcano. Between January and August 2003, a paroxysmal eruption occurred. As a result, some communities living around the volcano were evacuated (Webley et al., 2008). Between 1999 and 2012, a large amount of fine ash was produced, and pyroclastic flows occurred. Also, on June 3, 2018, a larger explosion occurred, with an eruption column up to 15 km amsl. As a result of the pyroclastic flow advancing in a

southeast direction (at Las Lajas barranca), a bridge was destroyed and many people lost their lives (Naismith et al., 2019).

As well as primary hazards, frequent and strong lahars are formed through the combination of pyroclastic material accumulated around Fuego and heavy rains. Lahar flows can reach a width of 40 metres, a depth of 4 metres, and a speed of > 8 m/s (Escobar- Wolf, 2013). These flows are very destructive, cause many injuries and fatalities, and regularly close the roads (Table 1). The scout camp mentioned earlier is an example. Besides the materials produced during the Fuego volcano eruption, pyroclastic materials that have previously accumulated around the volcano can also increase the volume and therefore destructiveness of the lahar. A huge amount of pyroclastic material has accumulated since 2015, which poses a significant risk to life, land and property (Naismith et al., 2019).

Table 1. Recorded lahars at Fuego volcano, especially in barranca Ceniza.

Date	**The barrancas where lahar flows occur**	**Source**
13.06.2008	Lahars have occurred in Santa Teresa and Ceniza.	GVP, 2009, 34:12.
20.06.2008	A lahar flow occurred in Ceniza. Blocks between 0.5 and 1 metre were dragged.	
04.07.2008	Lahar flows in the Ceniza barranca.	
21.05.2009	Lahar streams occurred in the Santa Teresa and Ceniza barrancas. 2-metre blocks were transported in the lahar flow.	
20.04.2010	Santa Teresa, Taniluya, Ceniza, Las Lajas, and El Jute	GVP, 2011, 36:6.
30.04.2010	Santa Teresa, Taniluya, Ceniza, Las Lajas, and El Jute	
29.05.2010	As a result of tropical storm Agatha, lahar flows occurred in the barrancas of Santa Teresa, Taniluya, Ceniza, Las Lajas, and El Jute.	
16.06.2010	Santa Teresa, Taniluya, Ceniza, Las Lajas, and El Jute	
21.09.2010	Santa Teresa, Taniluya, Ceniza, Las Lajas, and El Jute	
02.10.2010	Santa Teresa, Taniluya, Ceniza, Las Lajas, and El Jute	
13.09.2012 - 14.09.2012	According to the first evaluations made by INSIVUMEH, approximately 14 million m^3 of material has been mobilized in Ceniza.	GVP, 2013, 38:5.
01.06.2012	Ceniza, Trinidad, and Taniluya	
27.09.2012		
03.10.2012		
01.02.2013	Taniluya, Ceniza, Santa Teresa, Las Lajas, and Trinidad	
02.06.2013	Lahar flows in Ceniza -no damage and risk	GVP, 2014, 39:4.
08.06.2013	Lahar flows have occurred in Las Lajas (SE), El Jute (SE), & Ceniza (SSW).	
17.08.2013	Las Lajas, Ceniza (SSW) and, El Jute (SE). Lahar width: 30 m. Blocks were transported in the lahar flow.	
05.06.2014	Honda (E), El Jute (SE), Ceniza (SSW) and Santa Teresa (S). 1.5-metre blocks were dragged.	

Date	The barrancas where lahar flows occur	Source
02.09.2014	Lahars have occurred in Ceniza and Santa Teresa drainages. Also, weak avalanches were experienced in the Ceniza, Trinidad, Santa Teresa, Las Lajas, and Honda barrancas.	GVP, 2017, 42:5.
17-21 March 2017	Lahar flows were reported in Ceniza, Las Lajas and Santa Teresa. The La Rochela road was cut off for a couple of days.	GVP, 2017, 42:11
20, 23, and 24 April 2017	As a result of rain and snowfall, a lahar flow occurred in Ceniza on 20 April. Subsequent, lahar flows occurred in Ceniza, Santa Teresa, Las Lajas and Trinidad barrancas on April 23 due to 160 mm rain falling in three days.	
01.05.2017	Major lahars occurred in the Ceniza barranca. Blocks of nearly one-metre in diameter were transported in the lahar flow.	
04.05.2017	Lahar flows were reported in Ceniza, El Jute, Las Lajas and Trinidad. According to the estimates of INSIVUMEH, approximately 14 million cubic metres of material were emplaced in barrancas as a result of a pyroclastic flow.	
14.05.2017	Fine-grained material, similar to the consistency of concrete, and blocks of up to one metre, in diameter were carried into the Ceniza barranca.	
01.06.2017	As a result of the daily eruptions in the Fuego volcano, the movement of blocks and lahars have been reported.	
25.08.2017	Lahars occurred in Ceniza, Las Lajas and El Jute. The width of the lahar in Ceniza was 25 metres and its depth was three metres. Blocks of up to two metres in diameter were transported with the lahar flow.	GVP, 2018, 43:2.
03.09.2017	Due to heavy rainfall (1.059 mm) in September, seven lahars occurred (on 3, 4, 5, 6, 8, 27, and 29 September). Blocks with a diameter of about three metres were moved. Many roads were damaged.	
09.04.2018 and 22.05.2018	Lahars occurred several times in the second quarter of the year. Usually, these lahar flows were 20-30 metres wide and 1-2 metres deep. The diameter of the transported blocks was about 1-2 metres.	GVP, 2018, 43:8.
02.06.2018	Lahars occurred in the Ceniza, Trinidad, and El Jute barrancas. CONRED (The National Coordination for Disaster Reduction of Guatemala) raised the alarm level to red for the settlements of Escuintla, Santa Lucía Cotzumalguapa, Sacatepéquez, Yepocapa, Alotenango and Chimaltenango, located close to the volcano. As a result of this volcanic activity, 3271 people were evacuated, and 70 people died. A state of emergency was declared in the states of Escuintla, Sacatepéquez and Chimaltenango.	

Date	The barrancas where lahar flows occur	Source
08.06.2018	Lahar flows occurred in the Ceniza and Taniluya barrancas. The lahar width was 30 m and, the depth was 2-3 metres. Blocks of 2-3 metres in diameter were moved.	
10.06.2018	A lahar flow occurred in the Ceniza barranca. The lahar was 35 metres wide and three metres deep.	
12.06.2018	Lahars occurred in the Ceniza barranca, with a width of 20 metres and a depth of two metres. Blocks with a diameter of 1-3 metres were dragged.	
13.06.2018	Lahars were reported in the Ceniza barranca, with a width of 25 metres and a depth of two metres. Blocks with a diameter of 1-3 metres were dragged.	
14.06.2018	Lahars occurred in the Ceniza and Taniluya barrancas. The lahar width was 30-45 metres and the depth was three meters. Blocks with a diameter of three metres were dragged.	
15.06.2018	Lahars occurred in the Ceniza and Taniluya barrancas, with a width of 20-25 metres and a depth of two metres.	
20.06.2018	Lahars occurred in the Ceniza and Taniluya barrancas. The width was 30-35 metres and the depth was three metres. Blocks with a diameter of three metres were dragged.	
26.06.2018	Lahars were reported in the Ceniza barranca. Blocks with a diameter of 2-3 metres were dragged.	
30- 31 July, 2- 9 August 2018	Lahars have occurred in the Ceniza, El Jute, Las Lajas and Taniluya barrancas on 30 and 31 July, and 2 and 9 August. Blocks of 2-3 metres in diameter were dragged with the hot lahars.	GVP, 2019, 44:4.
29.08.2018, 21 and 27 September 2018	Lahars were reported in the Ceniza, Honda, El Jute, Las Lajas, Taniluya, Santa Teresa barrancas.	
13.10.2018	Lahars were reported in the Ceniza barranca. The lahar width was 30 metres and the depth was two metres. Blocks with a diameter of two metres were dragged.	
9-11 April 2019	Nine lahars were reported in the Ceniza, Las Lajas, El Jute, and Taniluya barrancas. The largest flows were 20 metres wide and three metres deep. Blocks with a diameter of 3 metres were dragged.	GVP, 2019, 44:10
18.04.2019	Two lahars were reported in the Ceniza and Taniluya barrancas.	
3, 14, 16, 20, 23, and 27-29 May 2019	In May, many lahars occurred in Las Lajas, Ceniza and El Jute barrancas. Blocks of three metres in diameter were moved.	
01.06.2019	Many lahars were reported in the Las Lajas, El Jute and Ceniza barrancas.	
13.08.2019	Many lahars were reported in the Santa Teresa, Las Lajas, El Jute and Ceniza barrancas. Lahar flows have caused damage to the roads between Siquinala and San Andres Osuna, and El Rodeo and El Zapote regions.	
17-20 August 2019	Many lahars were reported in the Las Lajas and Ceniza barrancas.	

2.3. Hydrology

Topographic Wetness Index (TWI) enables the study of the spatial scale effects of hydrological processes. It is possible to determine the flows affecting a point defined by the TWI and the areas where these flows accumulate.TWI is calculated by modelling the flows that can occur on the surface and subsurface depending on the topographic control. This study aims to determine the streams and the catchment area that will affect the lahar volume in the Ceniza barranca. This measurement is prepared based on the following calculation:

$TWI = Ln(\alpha / \tan\beta)$ (1)

In the equation, Ln is the natural logarithm, tan β is the slope of the cell, and α is the local area for a calculation (Cando-Jácome and Martínez-Graña, 2019).

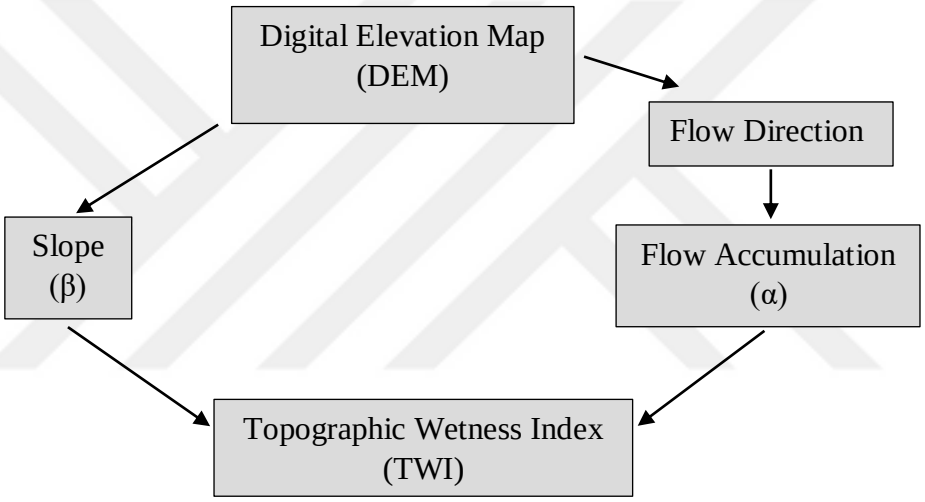

Figure 2.3. Steps to create the TWI

The topographic wetness index of the Fuego volcano and its surroundings have been obtained by applying the process steps in Equation 1 and Figure 2.3. For this, SRTM (Shuttle Radar Topography Mission), an international research effort that obtains digital elevation models on a near-global scale to create a database of the earth's surface, was used as a model. The following steps were applied respectively to determine the numerical parameters and topographic wetness index used in the applications (Table 2).

Table 2. Calculation of topographic wetness index and used parameters

Steps	Used Parameters
1	Flow Direction
2	Obtaining flow accumulation from flow direction
3	Slope (Digital Elevation Model)

Steps	Used Parameters
4	Slope (DEM) * 1.570796 /90
5	Determining the slope according to the conditions, Con (slope> 0, tan (slope), 0.001)
6	Scaling of flow accummulation (F_a Scaled= (F_a+1) * Cell Size)
7	Determination of topographic wetness index, WTI= ln (F_a Scaled/ tan slope)

Thus, as a result of a lahar flow, the accumulation area where water can be collected in the Ceniza barranca was determined (Figure 2.4).

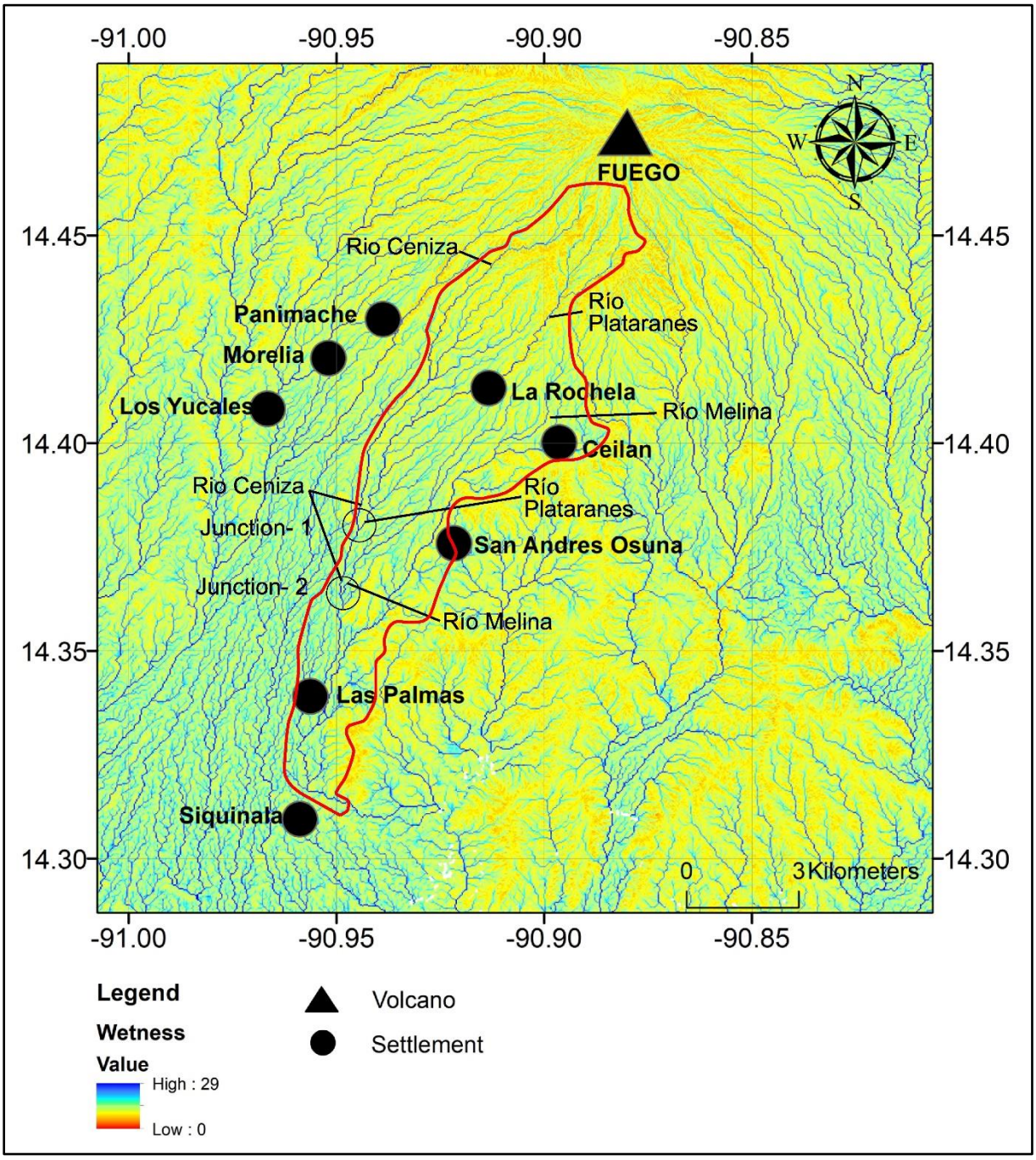

Figure 2.4. The catchment area in the Ceniza barranca (has prepared in the ArcGIS program).

The Ceniza drainage channel is a 73-kilometre channel, opening to the Pacific Ocean. There are many small (most of them seasonal) drainage channels in the study area, up to the Siquinala settlement, joining the Ceniza River (Figure 2.4). In lahar flows that may occur as a result of extreme rainfall, all these flows will be collected in Plataranes and Melina rivers, and they will be connected to the Ceniza channel at the junction 1 and 2.

3. Lahars

3.1. Rainfalls, Tropical Storms and Hurricanes

Conceptually, the currents that occur as a result of the rotation of air at low pressure are called a 'tropical cyclone'. Tropical cyclones with wind speeds of less than 39 miles per hour are called tropical depressions, and those that are faster than 39 miles are called 'storms'. When the maximum sustained speed of a storm reaches 74 miles per hour and above, it is called a 'hurricane'. Hurricanes are graded according to the Saffir-Simpson Hurricane scale with a number between one and five (Table 3), depending on the speed of the wind in the hurricane. The higher the category, the higher its destructiveness and the damage it causes (Kantha L., 2006; NOAA, 2013).

Table 3. Saffir-Simpson Hurricane scale (Kantha L., 2006).

Type	Pressure (m bar)	V_{max} (m/s)	Vmax (mph)
Tropical depression	1007	<17	<39
Tropical storm	<1000	17- 33	39- 73
Category 1	980	33- 42	74- 95
Category 2	979- 965	43-49	96- 110
Category 3	964- 945	50-58	111- 130
Category 4	944- 920	59-69	131- 155
Category 5	<920	>70	>156

Throughout history, Guatemala has been one of the Central American countries most affected by extreme rainfall, storms and hurricanes. Two weather events have occurred in the last 15 years leading to considerable material damage and loss of life. The first of these was Hurricane Stan in 2005, and the second was tropical storm Agatha in 2010. According to NOAA data, an average of twelve hurricanes/storms occur every year in the Atlantic basin. Due to these weather events, quite high amounts of precipitation are observed (as can be seen in Figure 3.1.A), and the effect of hazards are amplified. An example of this is the Pacaya volcano eruption, which

took place on May 27, 2010. Following this incident, a state of emergency was declared in the region, and schools were closed. As a result of tropical storm Agatha that occurred two days after the eruption, many lahars, landslides and floods took place, and the destructiveness of the disaster has increased even more, especially in Guatemala City where ashfall was remobilised by the heavy rain. Also, the Fuego 2018 eruption emplaced a significant amount of tephra over the summit, mostly as PDC deposits in the barrancas. This leads to the conclusion that similar disasters involving mass movements will occur at Fuego volcano, during the next tropical storm. For this reason, storms, precipitation periods, and the conditions necessary for triggering the lahar were analysed in this section.

The Fuego volcano is surrounded by the cities of Escuintla, Antigua and Chimaltenango. The Ceniza barranca is within the borders of Escuintla. There is an observation point called El Balsamo (14.28 N, -91.00 W), which is close to the study area and belongs to INSIVUMEH. According to the data received at this observation point, the annual temperature is between 20 degrees and 29 degrees, and the mean annual precipitation is about 3432 millimetres (Figure 3.1.A), a daily average of about 9.40 mm. This amount can increase about 30 times during storm periods (e.g. ~287.2 mm of precipitation occurred daily during tropical storm Agatha in 2010) and can cause lahars of a very high volume.

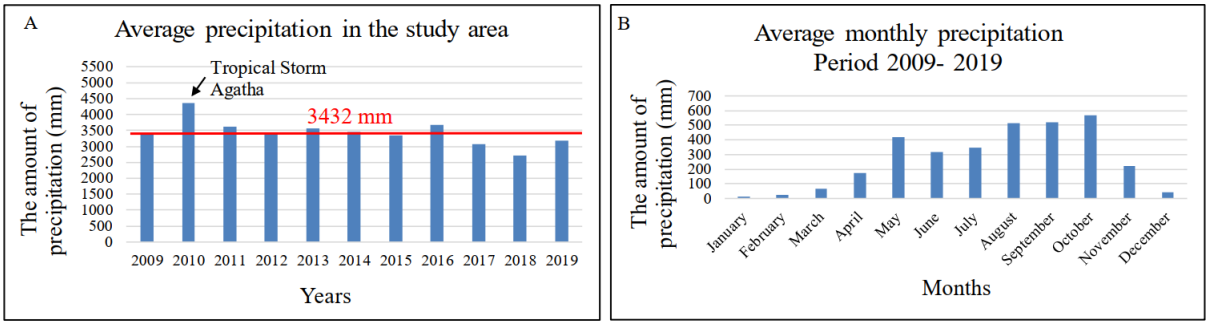

Figure 3.1. A. There was approximately 1000 mm more rainfall in 2010 due to tropical storm Agatha. (While the 11-year average precipitation was 3432 mm, there was about 4500 mm of precipitation during the Agatha storm). B. Distribution of precipitation between 2009 and 2019 by months.

The wet season occurs between May and November in Guatemala, with the highest amounts of precipitation in August, September and October (Figure 3.1.B). During this period, mass movements are regularly realised, and the ground can become water-saturated in Ceniza barranca, which has alluvial units around it at lower elevation (Figure 2.1). Also, according to NOAA data, the most intense period of storms and hurricanes is from mid-August and late

October. These storms, which may occur following extreme precipitation, will cause a high amount of material to move along the channel.

To limit the effects of lahars, it is important to determine the amount of precipitation that triggers them. In this way, when heavy rains occur, the public who live around the volcano can be warned and evacuated to minimize loss of life and property. For this purpose, we examined the last 32 lahars (Table 1) that occurred in the Ceniza barranca between 2 June 2018 and 20 August 2019. This period was chosen because the data are more precise. From the examination of the lahars that occurred between these dates, it was seen that lahars occurred during a minimum rainfall of 10.00 mm (approximately) (Figure 3.2.A).

Figure 3.2.B shows the graph of the rainfall between 29 and 30 May 2010 (tropical storm Agatha). While the amount of precipitation required for the occurrence of a lahar is 10.00 mm, many lahars have been reported because of the rainfall of 287.20 mm. As a result of this severe storm that started at night and continued until 9:00 a.m. (local time), there was loss of life and property. The BBC reported that 83 fatalities occurred and approximately 112,000 were displaced during the event.

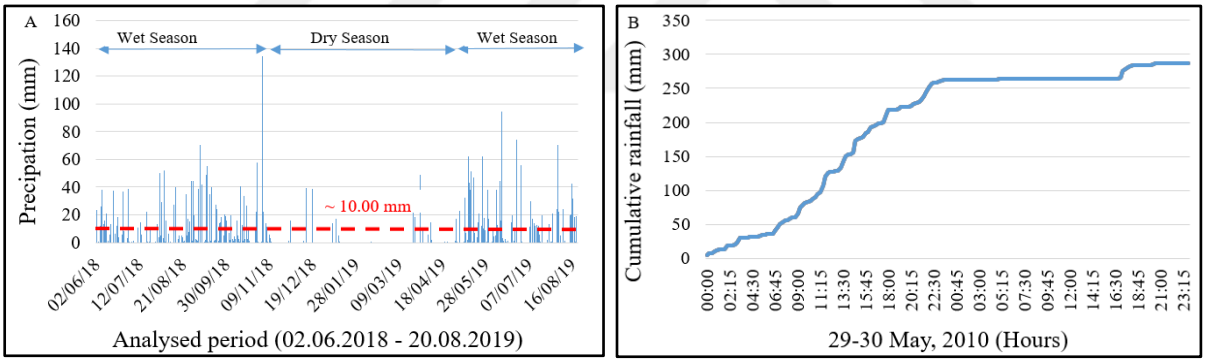

Figure 3.2. A. 10.00 mm of rainfall is required to trigger lahars in the Ceniza barranca. B. Change of precipitation during tropical storm Agatha depending on the hours. The amount of precipitation that started at midnight increased sharply until 22.30.

3.2. Lahar volumes used in the scenario-based study

Primarily lahars are mostly formed in a volume of 10^3 - 10^5 m^3 (Cando-Jácome and Martínez-Graña, 2019). As mentioned in the section on geological structure, there are geological units that can quickly erode (Figure 3.3) in the Ceniza barranca, and Guatemala is exposed to much heavy rainfall throughout the year. As a result of these precipitations, geological units and pyroclastic materials that merge with water may easily erode and may cause large mass movements.

As mentioned in the geological structure section, as a result of the eruptions in 1999 and 2012, approximately $5.24x10^7$ m^3 of pyroclastic material accumulated around the volcano (Naismith et al., 2019). In the 2018 eruption, approximately $3x10^7$ m^3 of the material was revealed (Pardini et al., 2019). Considering these conditions, a lahar flow of 10^7 and 10^8 m^3 may occur under the worst conditions. To evaluate the effects, a lahar flow of 10^6 m^3, and considering the worst-case scenario, the effects of lahar that could occur in a volume of 10^9 m^3 were evaluated.

Figure 3.3. A view from ~13 km south / southwest of the Fuego volcano. Eroded and decomposed alluvion units (GVP, 2013).

4. Lahar Modelling in the Ceniza Barranca

Within the scope of this study, the aim is to model lahar flows that may occur in the Ceniza drainage channel, under tropical storm conditions. The Laharz and Laharflow programs were used to measure the effects of lahar on the settlements along this channel route.

4.1. Laharz

Iverson et al. (1998) developed the Laharz program to define lahar flows. For this, they analysed 27 lahar paths at nine different volcanoes. The program is significant for providing results in a short time, being objective, repeating the analysis, and forecasting without field observation.

The Laharz program is written in ArcInfo Macro Language. The program allows the user to enter the volume value, and as this volume value increases, the length and width of the lahar increase proportionally. The program relies on a certain amount of mass and volume to move in the slope direction, and it performs these movements according to the height value on the grids. Accordingly, in a lahar where the cross-sectional area is A, and the planimetric area is B, the flow is defined according to the following equation.

$A = \alpha_1 V^{2/3}$

$B = \alpha_2 V^{2/3}$ (2), α_1 and α_2 is the constant values (α_1=0.05, α_2=200)

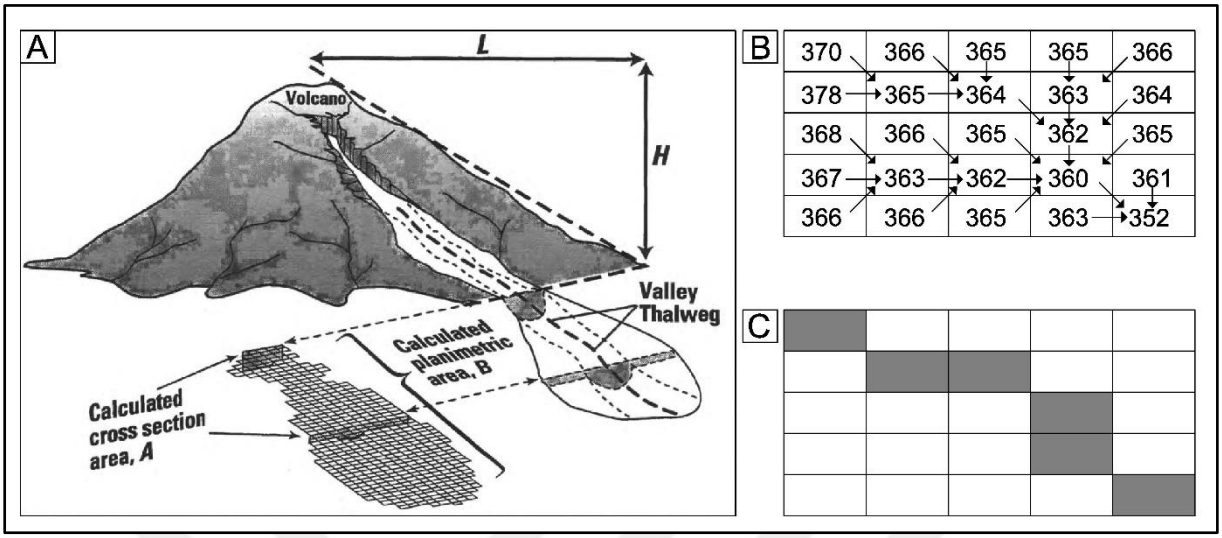

Figure 4.1. A. The size of cross-sectional and planimetric areas are determined by Laharz software. H denotes the vertical distance, L denotes the horizontal distance. The H / L ratio indicates the degree of hazard. **B.** Each cell is represented by a number value in the DEM (Digital Elevation Map). **C.** The flow direction will be like this, depending on the height values in B. This figure has been adapted from Iverson et al., 1998.

For the studies, the coordinates of the Fuego volcano and its surroundings were entered and the digital elevation model (DEM) was provided online (https://earthexplorer.usgs.gov). As seen in Figure 4.1, the resolution of DEM is of great importance since a flow in the Laharz software acts cellularly. For this reason, the highest resolution DEM was chosen, and then this selected DEM was coordinated in the ArcGIS program. In this study, the WGS-84 coordinate system was used.

In the first step, flow direction and accumulation in the study area have defined and the raster data obtained in ArcGIS have been converted to ASCII format for use in Matlab program. As mentioned earlier, within the scope of this scenario-based study, 10^6 10^7, 10^8 and 10^9 m^3 lahar volumes were entered (these volume values are described in section 3.2), and the areas affected by lahars in the planimetric and cross-sectional areas were determined. In this study, all possible flows have been evaluated, but the effects on the Ceniza drainage channel have been examined in detail. For this purpose, the slope map of the study area has also been prepared block movements will be intense in areas where the slope is high. Besides, in regions where the slope

is low, sedimentation and accumulation will be high, so these areas also needed to be determined. The possible flows are shown on the terrain modelled in 3D (Figure 4.2).

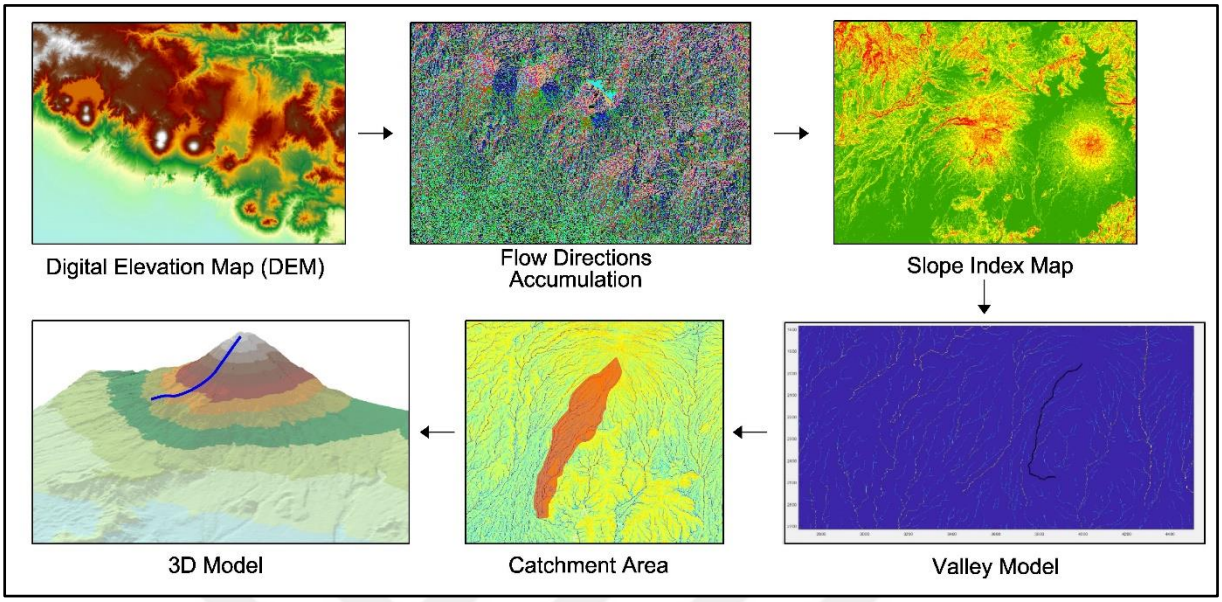

Figure 4.2. The order of displaying the lahar data obtained using Laharz and Matlab software in the ArcGIS program.

The steps shown in Figure 4.2 are carried out by taking into account the pre-existing topography, geological structure, and hydrology in the region. One of the most critical steps after these studies is determining the intensity of the hazard. Lahars will be devastating along the routes it passes directly, and this degree of risk will decrease as we move away laterally from the flow. Since the presence of a hazard is measured by its impact on people, identifying the people and structures that will be exposed to the hazard is another significant issue. Also, in a possible warning, the disappearance of evacuation routes or junctions can further increase the degree of disaster. For this reason, the study focuses on the settlements and structures that will be affected. Also, a risk map has been created by determining the area of impact (Figure 4.3).

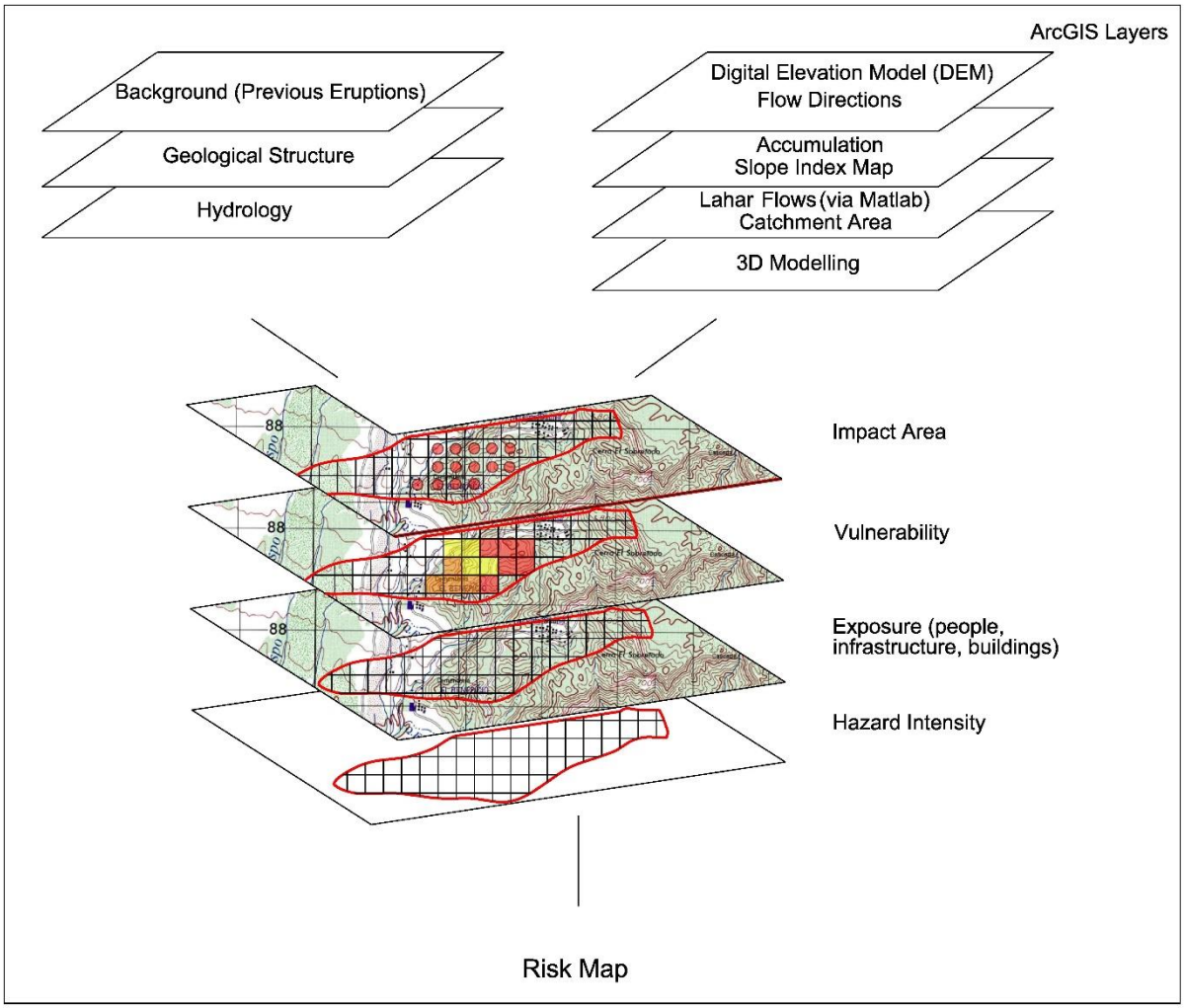

Figure 4.3. General scheme of studies with Laharz

4.1.1. Lahar models in Laharz

To understand the hazard of lahars that may occur at Fuego, 56 points have been defined from the summit of the volcano. In this scenario-based study, 10^6, 10^7 and 10^8 m^3 (as explained in section 3.2) lahar volume values were entered (Figure 4.4). The effect of a 10^9 m^3 lahar flow has been evaluated in Figure 4.5 since a greater area was covered.

As illustrated in Figure 4.4, when all lahar flows that may occur in seven barrancas are evaluated, an area of 300 km^2 will be affected (it is calculated on the coordinated ArcGIS map). These are the settlements of Santa Lucía Cotzumalguapa, Panimache, Las Palmas, Siquinala and Escuintla and the villages connected to these settlements.

Three rivers feed the Ceniza barranca, namely the Rio Ceniza, Rio, Plataranes and Rio Melina (Figure 2.4). Using the Laharz and Matlab software, a 106 m3 volume of lahar flow is expected

to be effective for approximately 10 km. This lahar will take place within the Ceniza channel, and the stream is not expected to overflow laterally.

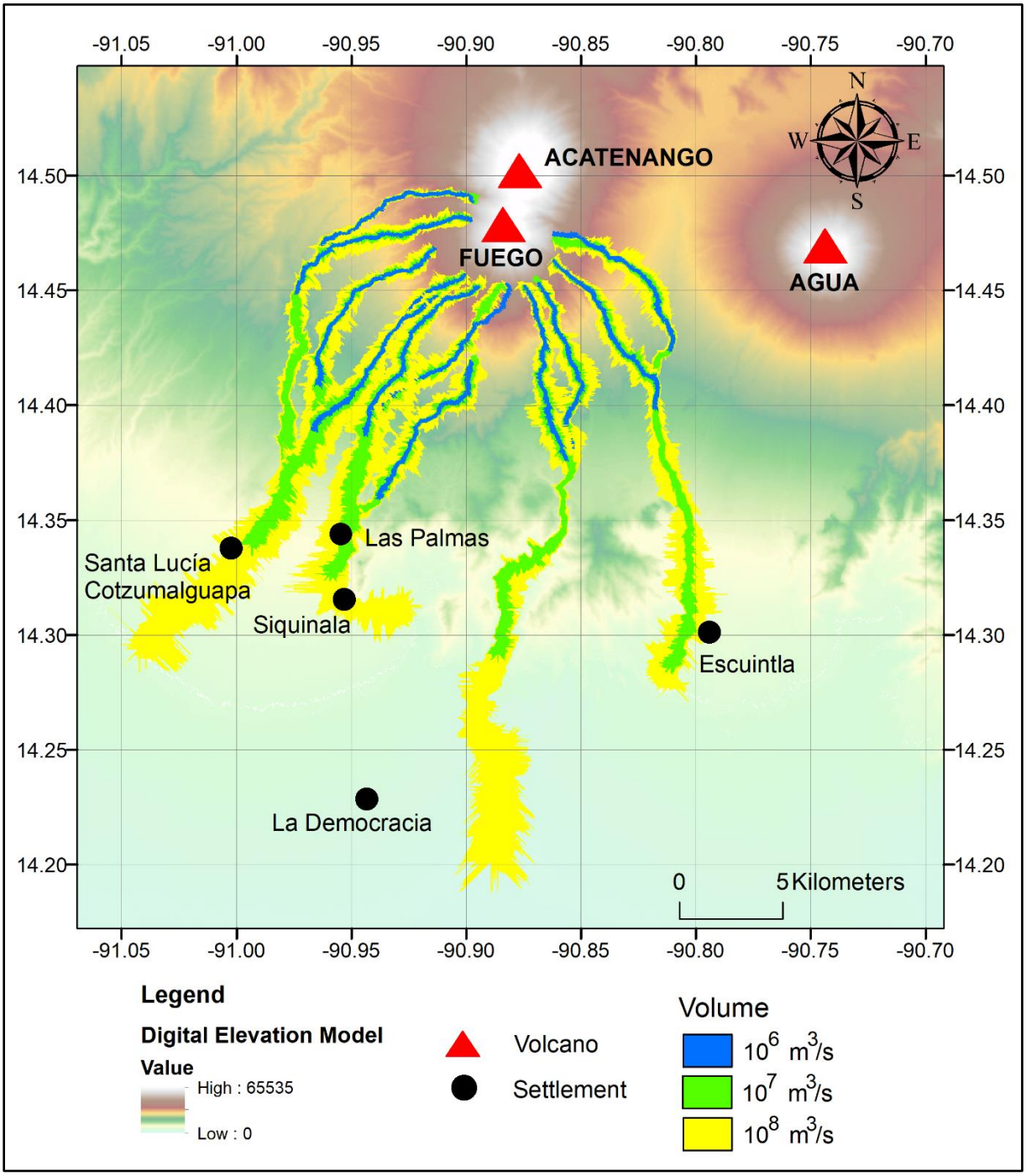

Figure 4.4. Areas to be affected if a lahar flow of 10^6 to 10^8 m^3 volume occurs in the Fuego volcano.

A lahar flow that may occur in a volume of 10^7 m^3 will be active along a line of approximately 17 km, and it will affect the Las Palmas settlement on this route.

If a 10^8 m^3 volume lahar flow occurs in an area between the Taniluya and Ceniza barrancas, it will also have a devastating effect on the Panimache settlement since it is expected to have a lateral expansion in the barrancas.

In a flow of 10^8 m^3, the lahar will flow towards the east in the Siquinala region. The significant point is that it will overflow from the bed in the Siquinala region, and will move into the settlement centre (Figure 4.5).

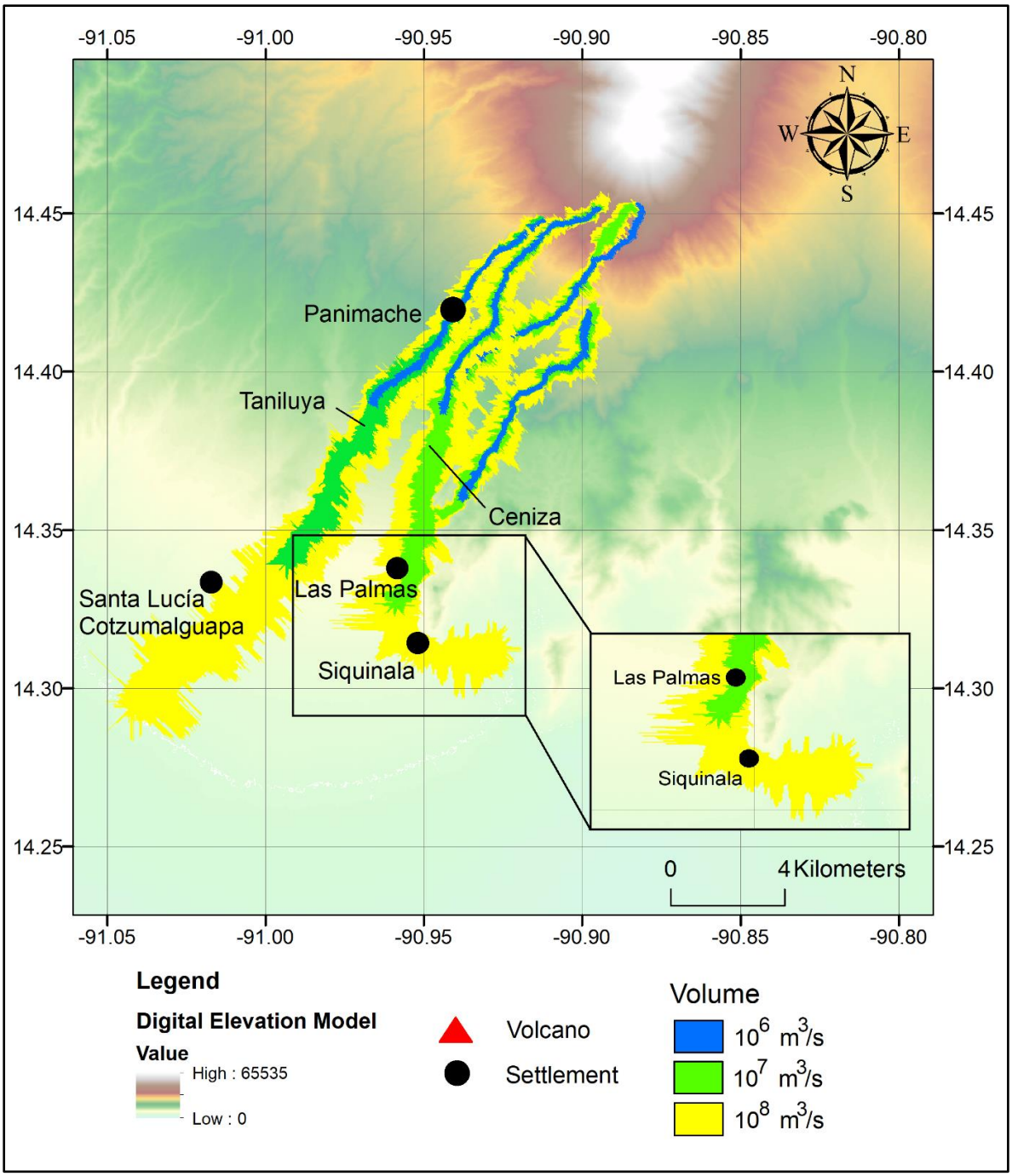

Figure 4.5. Areas to be affected in the lahar that may occur in a volume of 10^6 to 10^8 m^3 in the Ceniza channel

A lahar with a volume of 10^9 m^3 would affect an area of 23 km long and up to 7 km wide (between Las Palmas and Santa Lucíia Cotzumalguapa settlements). In this scenario, superficial flows are expected to occur in the areas between the Taniluya and Ceniza barrancas, and the flows occurring in both channels are also expected to merge. In this case, a lahar would affect all the Las Palmas and Siquinala settlements, and most of the Panimache and Santa Lucía Cotzumalguapa settlements (Figure 4.6). The destructive effects caused by lahars (on infrastructure and people living in the region) were evaluated in the section of the affected area.

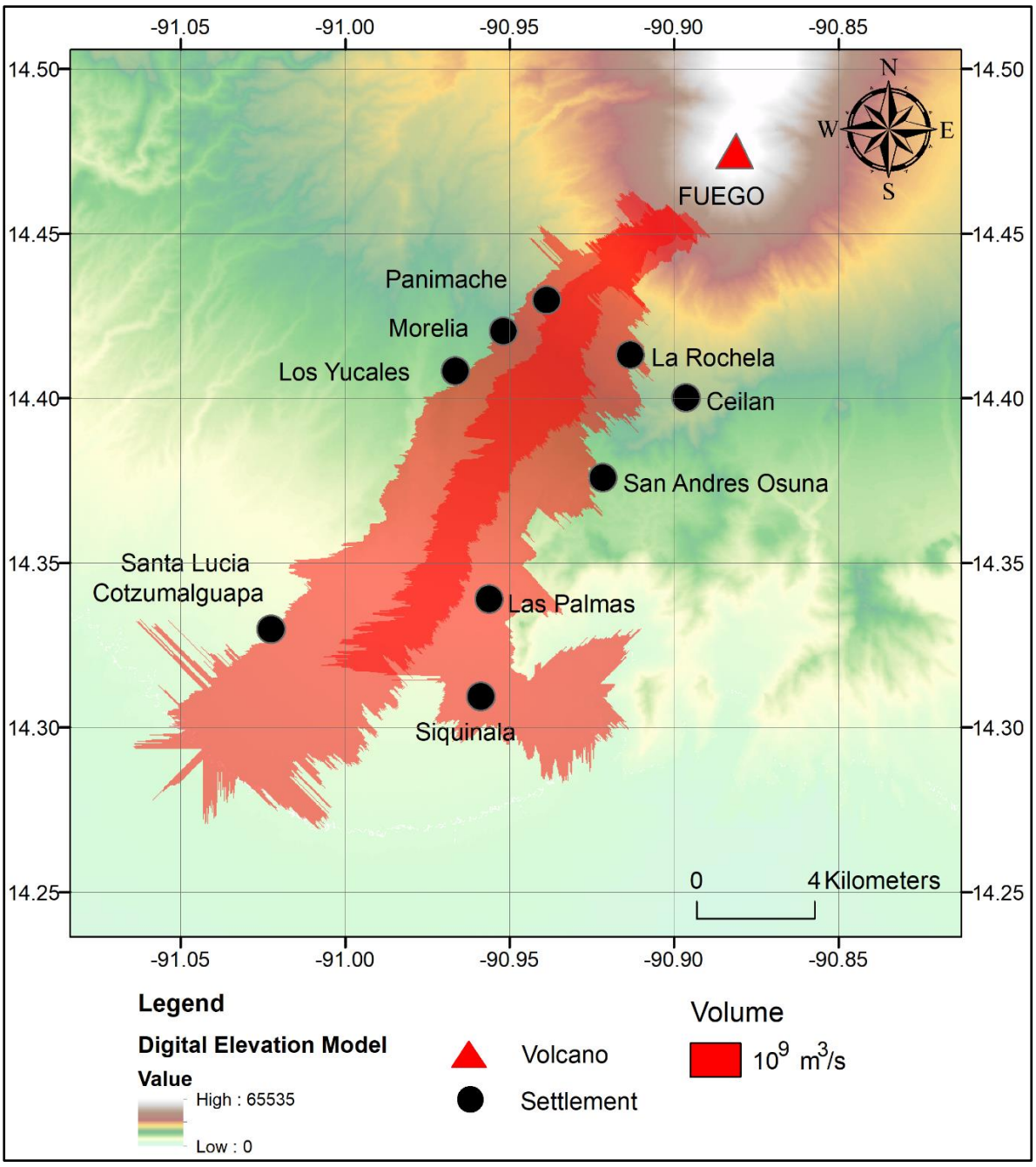

Figure 4.6. Areas that can be affected by a lahar flow with a volume of 10^9 m^3

4.2. LaharFlow

LaharFlow is software that models flow in topography. The mathematic model is based on fluid mechanics, accumulation and erosion morphodynamics, and granular dynamics (Woodhouse et al., 2016). There is no need to download a program for the software; it is possible to produce models through a dedicated web interface.

One of the most critical factors that determine the movements of lahars is topography. LaharFlow uses the 30 m SRTM, which can be accessed globally for free as the digital elevation model. The DEM appears automatically when the coordinates of the desired area are entered. In the software, it is possible to display models in the direction of 40 km north to -south and 40 km east to -west. The software also enables its users to use digital elevation models (Woodhouse et al., 2016).

LaharFlow provides information on the depth, velocity, solid concentration, and densities of lahar flows. It contains the drag formulation between both liquid and solid particles, and this allows the flow regimes to be diversified (Woodhouse et al., 2016).

With LaharFlow, multiple streams can easily be examined, and it is reproducible. When the coordinate is entered, the digital elevation model is displayed automatically. Unlike the Laharz program, it is possible to obtain results in the specified simulation time. This time is a maximum of 18000 seconds, which is five hours (Figure 4.7).

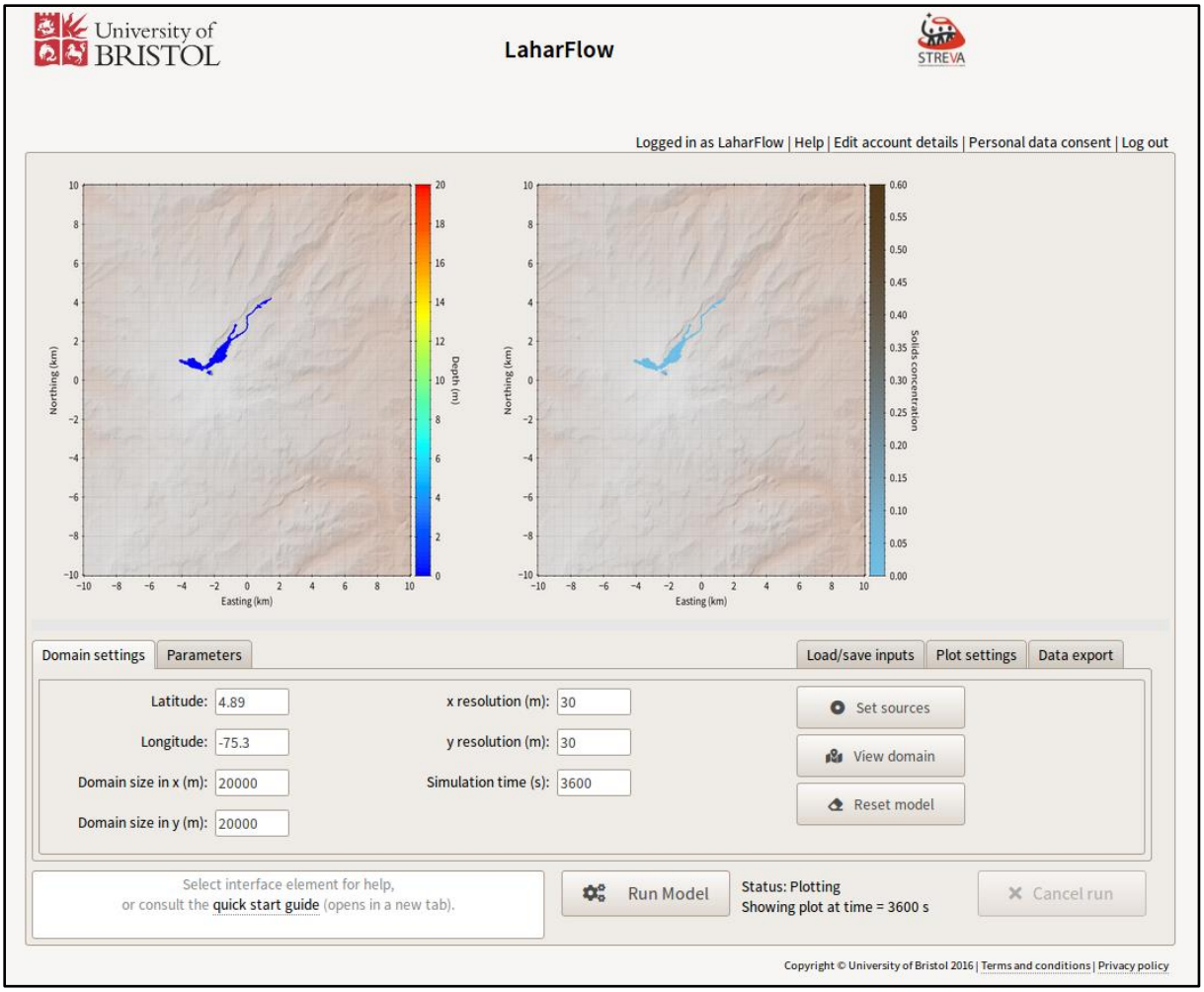

Figure 4.7. The interface of LaharFlow (https://www.laharflow.bris.ac.uk/help/quickstart/)

In LaharFlow, many parameter values can be determined by the user, which allows the user to obtain a better model based on field observations. These parameters are the Chezy coefficient, granular friction, friction switch value and rate, erosion rate and depth, bed porosity, and solid diameter. Also, it is possible to display the range and the maximum and minimum values of this range.

It is possible to add the properties of the flux and the cap sources for the lahar flows that may occur in LaharFlow. Adding the cap source allows more accurate modelling for lahar flows that may occur in volcanoes with glaciers or lakes at the summit. However, since there is no such formation at the top of Fuego, the cap source was not used.

While the points are selected manually in Laharz and Matlab for lahars, multiple streams can be defined by entering the coordinates of the streams in LaharFlow. It is also possible to determine the width in metres of the flows that may occur. The steps to be followed to detect the flows that may occur on the surface are shown in Figure 4.8.

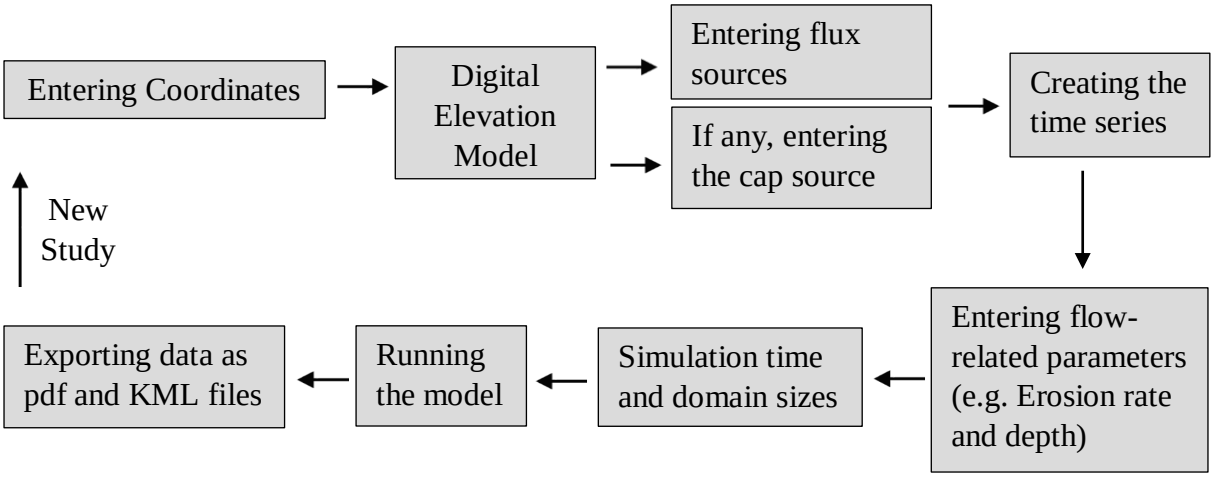

Figure 4.8. LaharFlow working principle and determination of lahars

The volume of flows is determined by entering time and volume flux values. The same volume values used in Laharz were entered in LaharFlow, namely, 10^6, 10^7, 10^8 and 10^9 m^3. For this, the formulation in LaharFlow is as follows:

$V = 0.5 * Q * T$ (3)

According to this formula,

Time: 0, 250, 2500

Volume Flux: 0, 800, 0

A volume of $V = 0.5 * 2500 * 800 = 10^6$ m^3 is obtained.

The graph of the flow that may occur in a lahar flow, where the solids concentration is also determined as 0, 0.2 and 0, respectively, is as follows.

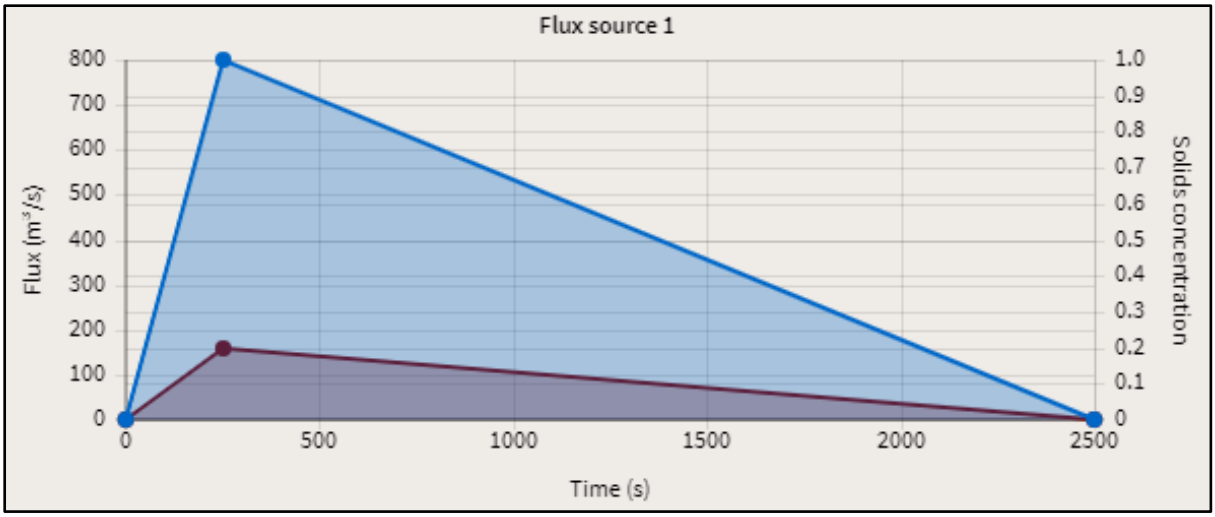

Figure 4.9. Graph of the flow that can occur in a lahar flow of 10^6 m^3. The area in red shows the change in solids concentration, while the area in blue shows the change in flux.

Lahar flows that can occur at 10^6, 10^7, 10^8 and 10^9 m^3 volume values in LaharFlow have been modelled by using the above equations and parameters.

After all the processes are completed, a pdf file containing all the results can be downloaded (the map of flow depth and speed, the map of flow concentration and density, and the map of the change in elevation) (Appendicies-1). In addition, KML files are provided to display lahar flows on Google Earth. Accordingly, the flows that may occur at the volume values defined at Fuego volcano are as follows.

4.2.1. Lahar models in LaharFlow

As can be seen in Figure 4.10, when a lahar flow of 10^6 m^3/s takes place in the Ceniza drainage channel, it will pass a distance of about 12 km (from the peak of the volcano). As a result of this volume of lahar flow, no damage is expected to the settlements. It is expected that agricultural areas will be damaged if the channel overflows laterally.

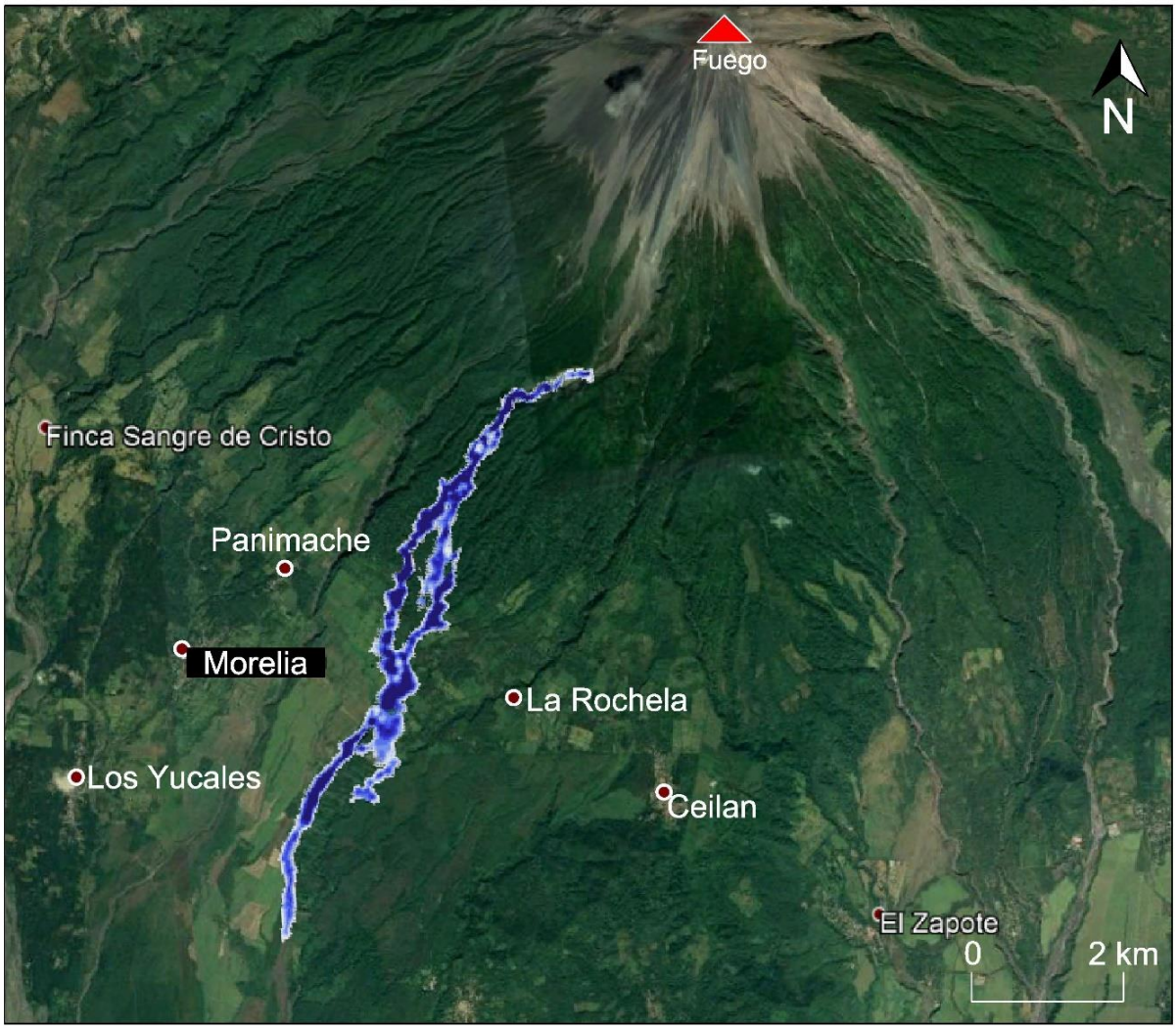

Figure 4.10. The motion of lahars in volumes of 10^6 m^3/s in the Ceniza channel (on Laharflow program). Blue areas indicate the areas that could be submerged.

At a lahar flow of 10^7 m^3, the flow will not be limited to the Ceniza barranca, and it is expected to diverge into the Taniluya barranca. This flow will partially affect the agricultural area of Panimache, Morelia and Los Yucales (Figure 4.11).

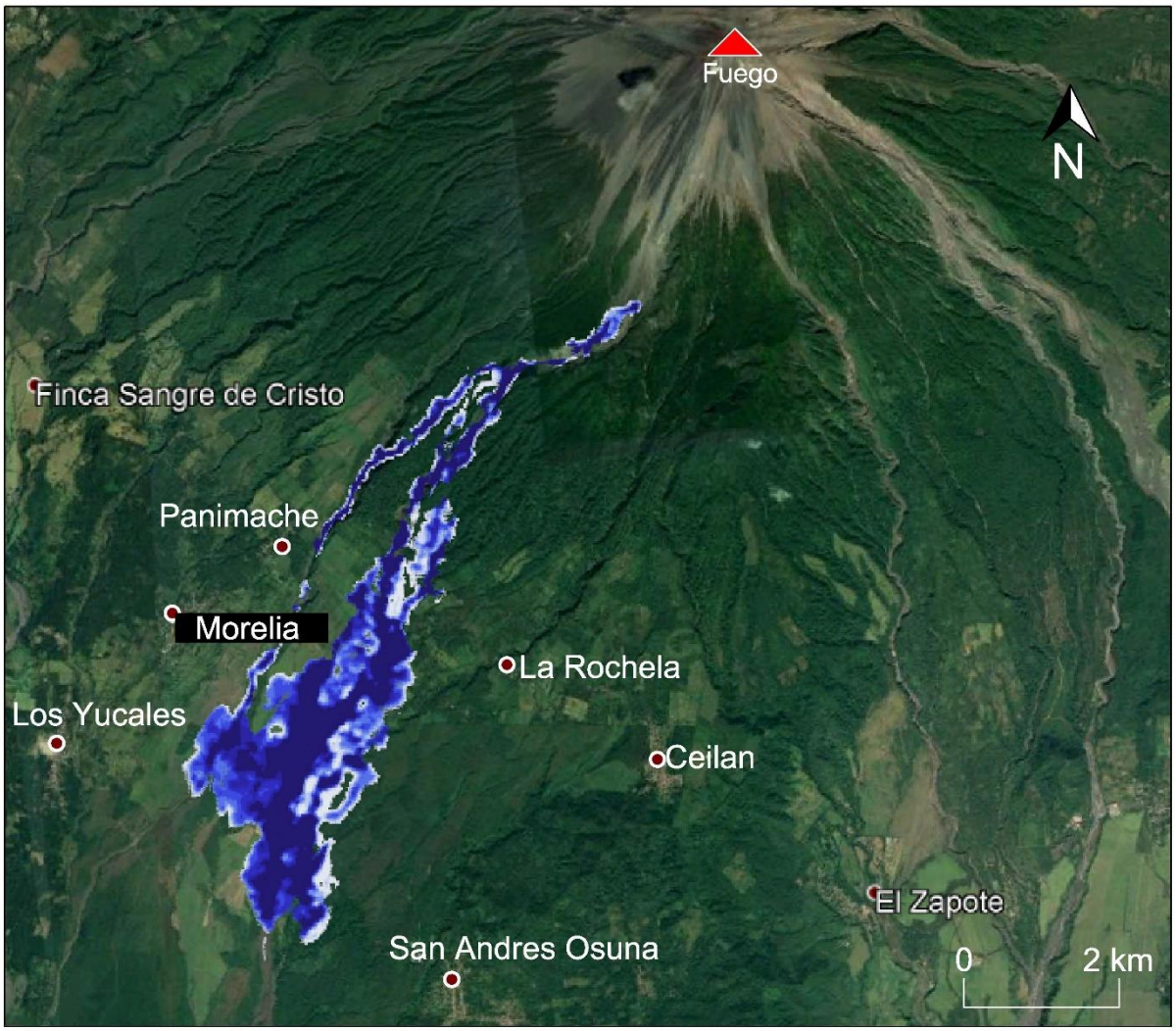

Figure 4.11. Areas that will be affected in a lahar flow of 10^7 m^3. Blue areas indicate the areas that can be submerged.

In a 10^8 m^3 lahar flow that may occur in the Ceniza channel, the Panimache region will be partly submerged (Figure 4.12). The most important reason for this is that the lahar mass, which is rapidly advancing in the Ceniza barranca, overflows from its bed and merges with the Taniluya barranca (Figure 1.1).

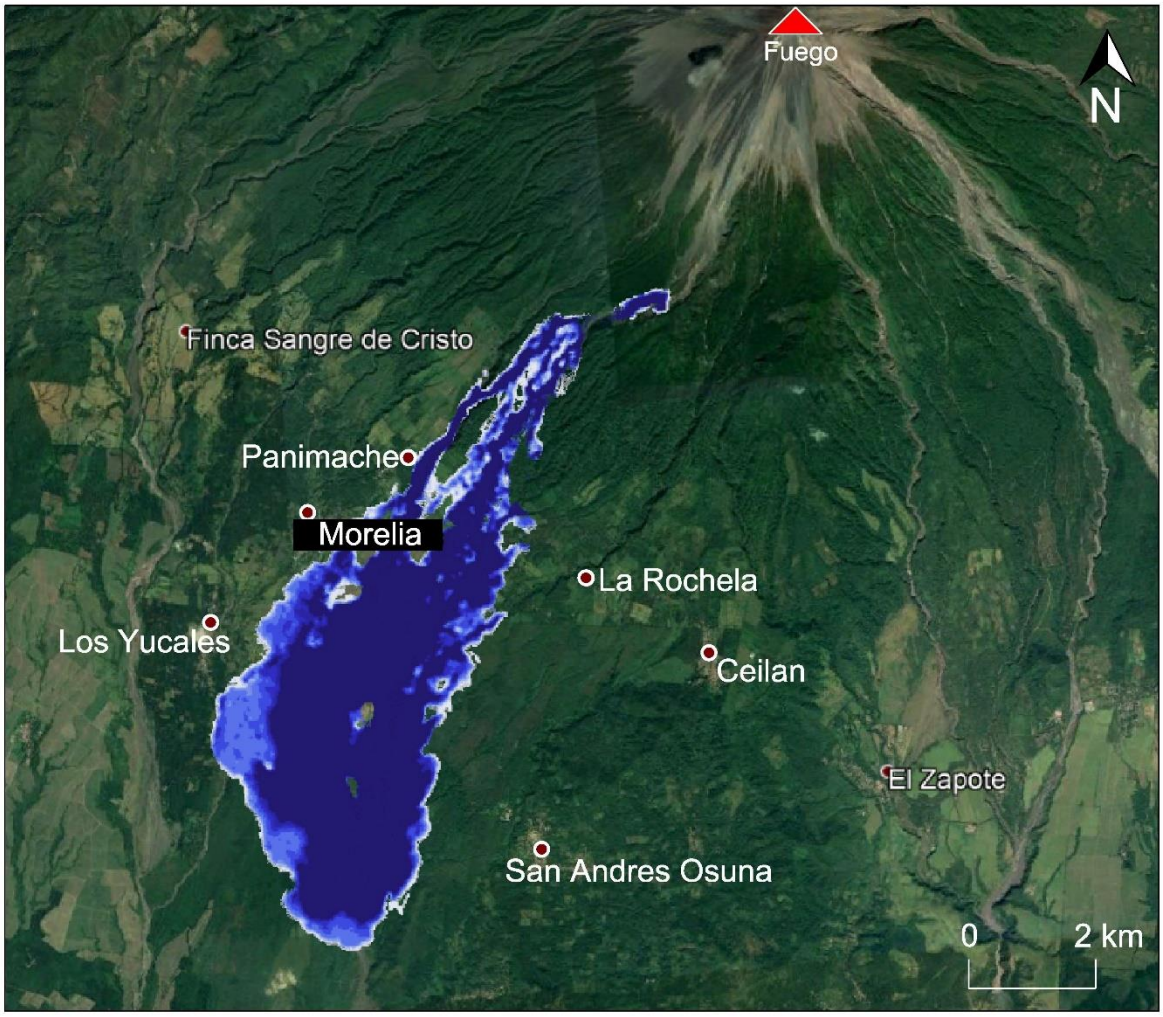

Figure 4.12. The areas that will be affected by the lahar flow of 10^8 m^3. Blue areas indicate the areas that would be submerged.

When the volume reaches 10^9 m^3, a lahar will move in three branches. The first is the flow that moves through the Ceniza barranca, which will cause the Las Palmas settlement to be submerged. The second is the lahar that flows through the Platanares and Melina rivers (Figure 2.4). As a result of this flow, a large part of La Rochela and San Andres Osuna settlements will be submerged. The third one is the flow that progresses in the Ceniza and Taniluya barrancas. In this lahar flow, the settlements of Panimache, Morelia and Los Yucales will be affected (Figure 4.13).

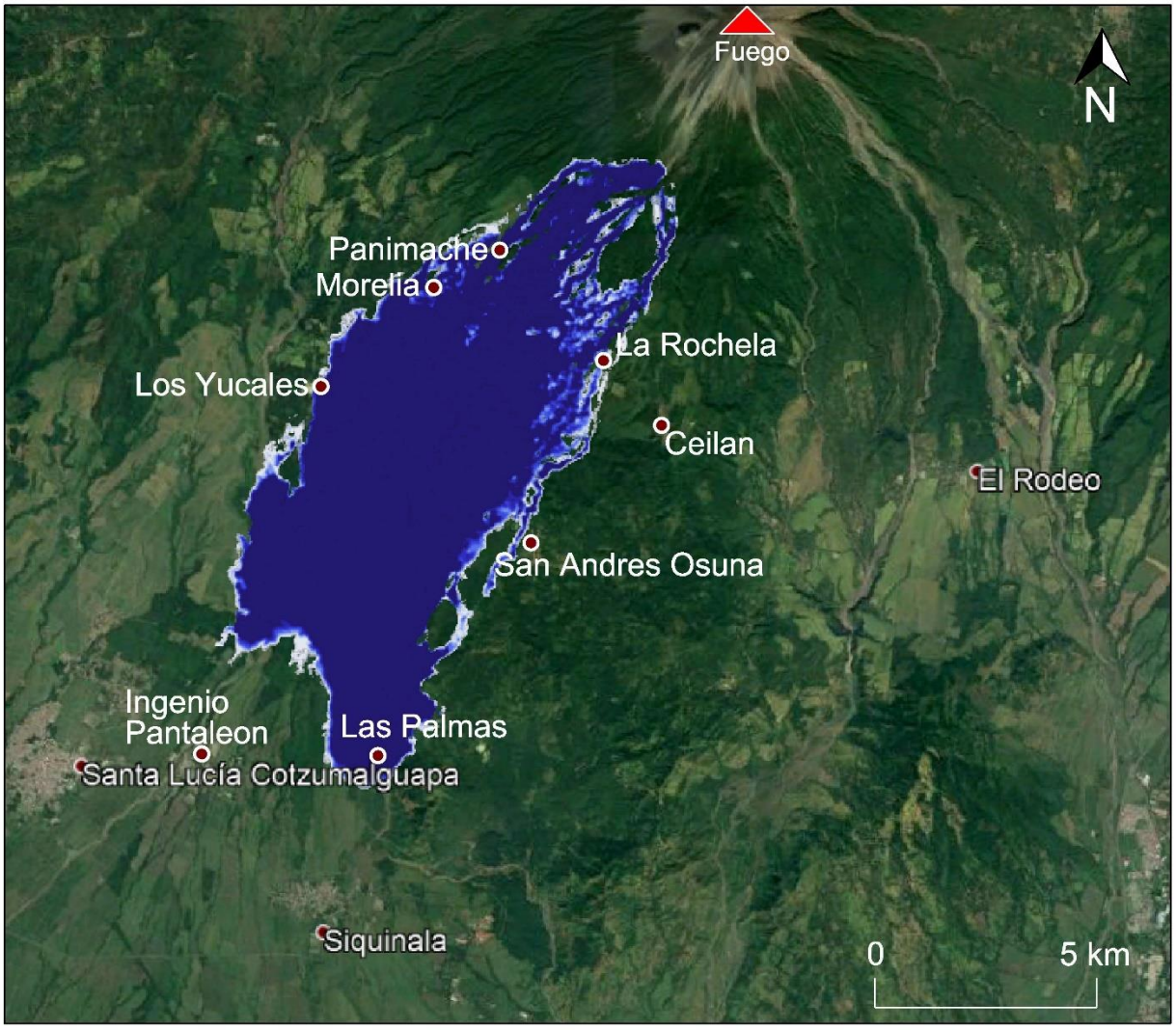

Figure 4.13. The areas that will be affected by the lahar flow of 10^9 m^3. Blue areas indicate the areas that can be submerged.

4.3. Affected areas and the evaluation of data

Lahar models in the Laharz and LaharFlow programs, their effects, the areas to be affected, and recommendations are given in Table 4. There are similarities in both programs and some differences. The factors that cause this are discussed in Part 5.

Table 4. Areas to be affected by lahar flows that can occur between 10^6 and 10^9 m^3/s, and recommendations

Used program	**Lahar Volume**	**The amount of area to be affected (km^2)**	**Inundated Area**	**Recommendations**
Laharz	10^6 m^3	1.95	The settlements are not expected to be damaged. The agricultural area remaining at the junction of the Ceniza and Plataranes rivers is expected to be submerged.	Although such a volume of lahar flow does not damage settlements, rolling of large blocks can pose a problem as mentioned in Table 1. For this reason, it will be useful to identify and remove blocks periodically that may pose a risk.
LaharFlow		2.65		
Laharz	10^7 m^3	8.00	In a lahar flow of this volume, it is expected that agricultural lands located near the Ceniza barranca will be damaged. It is also expected that lahars will move along the Platanares River and damage the surrounding agricultural lands. There is likely to be partial damage in the Las Palmas settlement. However, ragged edges are seen in the lahar flow affecting this settlement. This shows that there may be a problem, according to the DEM resolution.	In a lahar flow that can occur in this volume, the road connecting the El Rodeo and Siquinala will not be safe because it passes through the Ceniza channel. If there is no lahar trigger in the Las Lajas and Honda drainage channels, then it will be more advantageous to use El Rodeo and Escuintla roads for evacuations (No. 14 and CA9).

Used program	**Lahar Volume**	**The amount of area to be affected (km^2)**	**Inundated Area**	**Recommendations**
LaharFlow		8.55	In lahar modelling in LaharFlow, it is possible to see the flow progressing from three branches: (1) The flow that takes place in the Ceniza barranca, (2) the flow in the Taniluya barranca, and (3) the flow in the Platanares River. It is expected that agricultural lands will be damaged in all three flows. The LaharFlow model predicted that lahars would have an effect at wider and shorter distances than the distances predicted by Laharz.	
Laharz	10^8 m^3	26.50	Agricultural lands in the Panimache region and La Rochela, some parts of the San Andres Osuna settlement, and the whole of Las Palmas will be negatively affected by lahar flows. Also, some parts of the Siquinala region, with a population of approximately 30,000 (INDE, 2020), are expected to be inundated.	In response to a lahar flow of this volume, it is necessary to perform evacuations by using the El Rodeo and Escuintla roads.

Used program	**Lahar Volume**	**The amount of area to be affected (km^2)**	**Inundated Area**	**Recommendations**
LaharFlow		21.50	Unlike the observations above, it has been observed that the Las Palmas and Siquinala settlements will not be affected in the lahar flow modelling of 10^8 m^3 in LaharFlow. However, it is estimated that the Panimache settlement will be submerged.	
Laharz	10^9 m^3	77.00	In this most devastating scenario, the Panimache, La Rochela and San Andres Osuna, Las Palmas, and Siquinala settlements will be significantly affected. Besides, the Ingenio-Pantaleon settlement, between the Santa Lucía Cotzumalguapa and Siquinala settlements, will also be inundated.	In a rather large lahar volume of 10^9 m^3 /s, the affected area may be quite large. For this reason, alternative road routes should be created for evacuations.
LaharFlow		63.50	Unlike the modelling performed in LaharFlow, it is expected that the Morelia and Los Yucales settlements will be affected by the lahar flow, and the Ingenio-Pantaleon and Siquinala settlements are not expected to be affected.	

5. Discussion

In this study, Laharz and LaharFlow model outputs, determined using consistent flow volumes and topography, were compared. Firstly, the parameters used in both models were provided in this section. After that, both models were shown on a single figure to show the differences in the same volumes (Figure 5.1). Then, the advantages and disadvantages of both programs were analysed. Considering all these conditions, the impact area of a large volume lahar (between 10^6- 10^9 m^3) that will start during a tropical storm in the Ceniza barranca has been determined (Figure 5.2). In Table 4, recommendations were provided to minimize the effects of such a possible lahar.

The LaharFlow model provides the user with a wide range of output. It gives the depth, maximum, and average velocities of the flows at each point. It also provides a map of flows. Solid concentrations play a significant role in lahar flows; lahars with high fine grain content and that flow faster than 8 m/ s pose a particular threat. LaharFlow provides a detailed map of solids concentrations, and determines topographic changes and the amount of mass in each area. However, these outputs cannot be obtained from Laharz. It is possible to see runout and inundated areas as common features in Laharz and LaharFlow (Table 5).

Table 5. Comparison of the parameters that can be obtained with Laharz and LaharFlow

Parameters	Laharz	LaharFlow
Flow depth	×	✓
Maximum/Average velocity map	×	✓
Solid concentration	×	✓
Runout	✓	✓
Inundated area	✓	✓
Maximum height	×	✓
Elevation change	×	✓
Mass per unit area	×	✓

Significant differences were observed when Laharz and LaharFlow models were compared (Figure 5.1). This is because Laharz is a semi-empirical and statistical code (Vargas Franco et al., 2010). Iverson (2003), Sparks and Aspinal (2004) suggested that Laharz software could be an alternative to physical models with multi-parameters (Ogburn and Calder, 2017). LaharFlow is based on the mathematical model and calculations are based on shallow water equations. Also, LaharFlow is based on multiple parameters, as mentioned above.

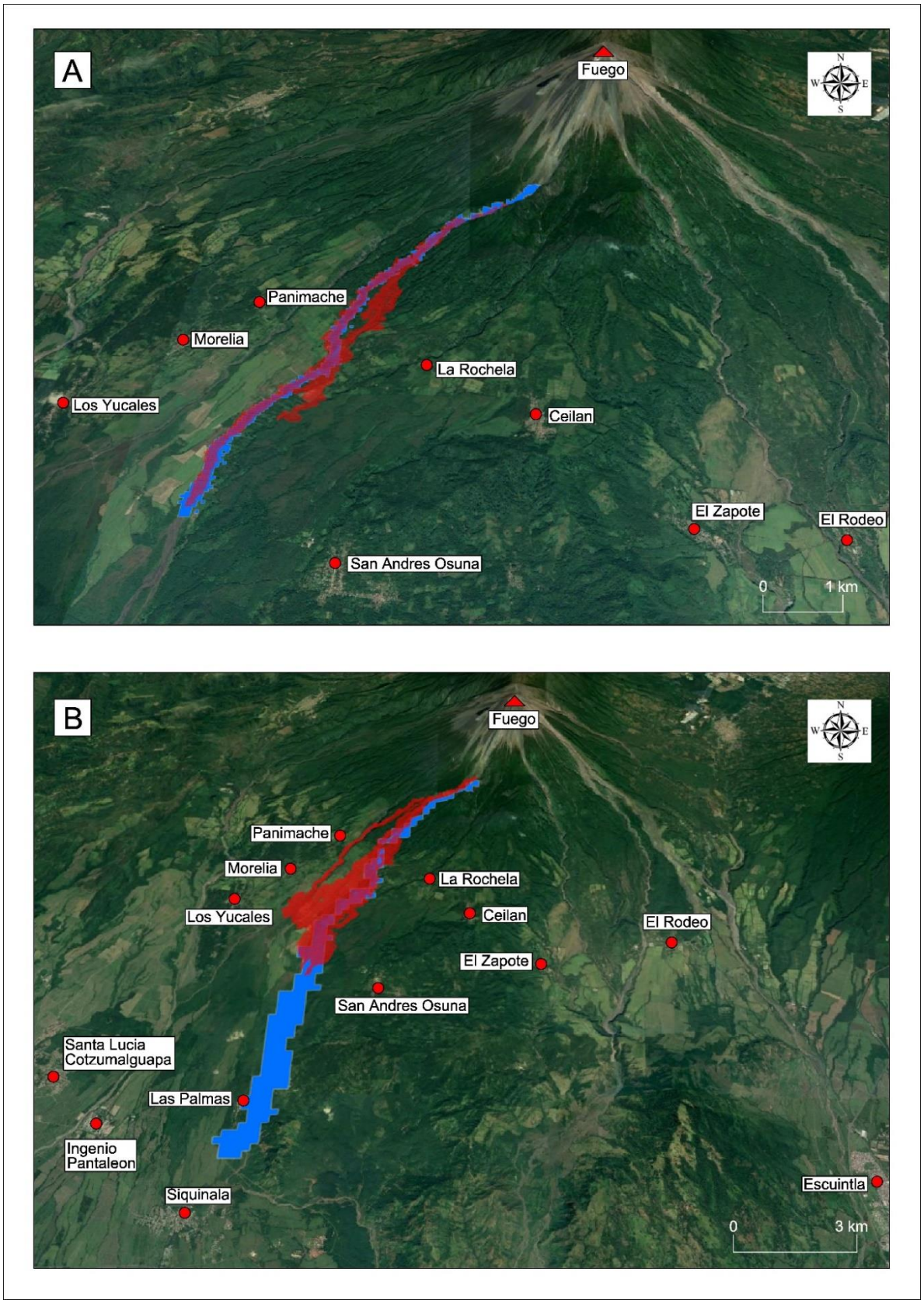

Figure 5.1. Comparison of flows occurring in Laharz and Laharflow. The lahar flow shown in blue is modelled in Laharz, while the areas shown in red are modelled in LaharFlow. A. 10^6 m^3, B. 10^7 m^3

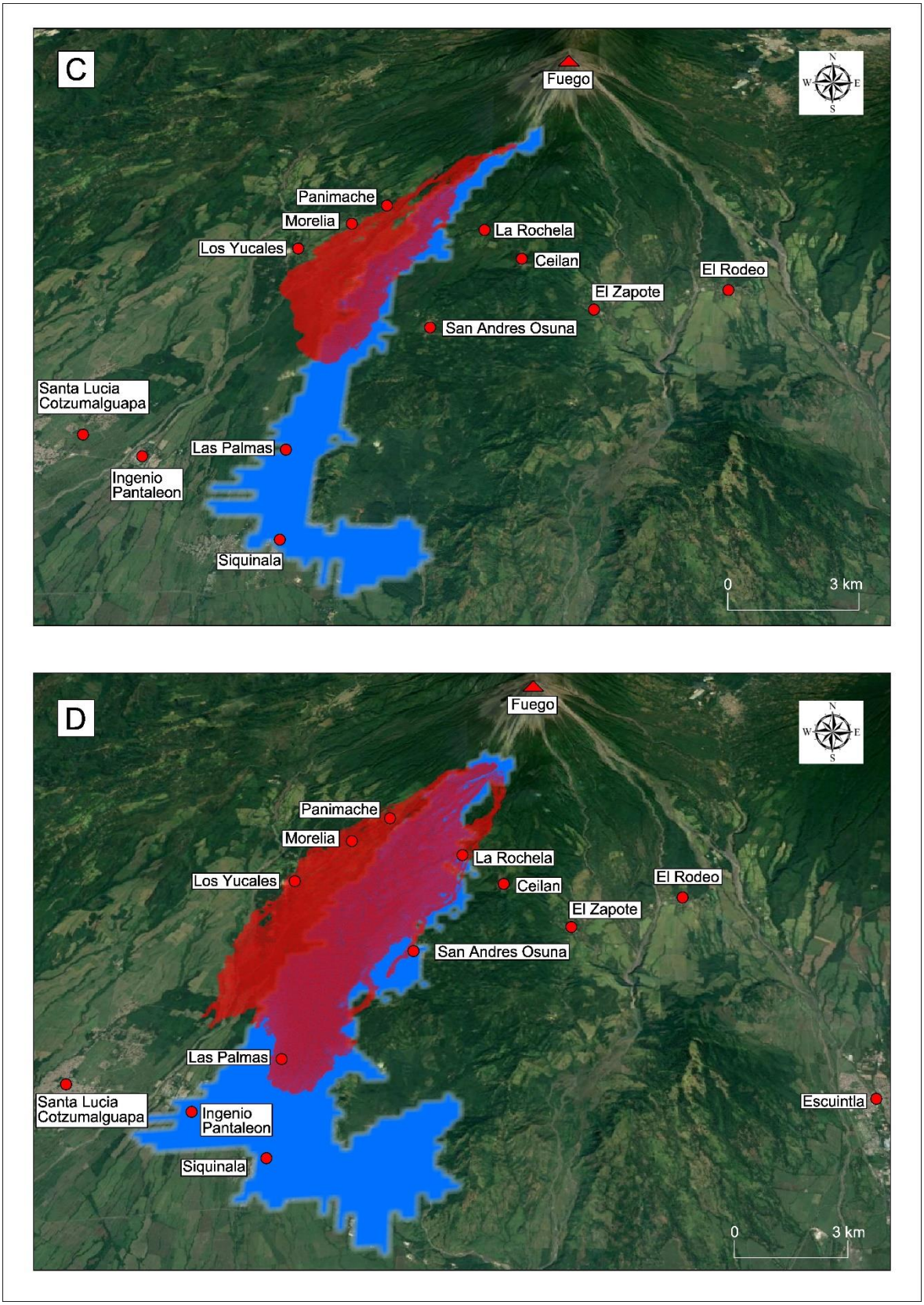

Figure 5.2. Comparison of flows occurring in Laharz and Laharflow. The lahar flow shown in blue is modelled in Laharz, while the areas shown in red are modelled in LaharFlow. C. 10^8 m^3, D. 10^9 m^3.

Another difference is that there are differences between the areas that will be affected by lahars (Table 4). 10^6 m^3 of lahar will affect an area of about 2 km^2. When this amount reaches 10^7 m3, an area of approximately 8 km^2 will be inundated. However, there are differences between the areas that will be affected when the volume increases to 108 and 109 m3. In the volume of 108 m3, it is expected to be effective on an area of 26.5 km^2 in Laharz, while it is 21.5 km^2 in Laharflow. When the volume reaches 109 m^3, an area of 77 km^2 is predicted to be inundated in Laharz whereas in Laharflow this area is 63.5 km^2. That is, as the volume increases, differences are observed between the amount of areas that will be affected.

The other difference between Laharz and LaharFlow is that Laharz creates a geometric flow. That is, it usually assumes that the lahar will run through a valley. For this reason, the lateral widths are narrower in Laharz, although the length is greater. In contrast, LaharFlow calculates many parameters, it moves in a lateral direction, and it calculates the new flow that may occur as a result of the flow passing to another channel. Therefore, LaharFlow also calculates new possibilities that may occur.

Considering the differences in all these models, the parameters used, and the working principle of the programs, the advantages and disadvantages of both programs are as follows (Table 6).

Table 6. Comparison of advantages and disadvantages of Laharz and LaharFlow programs

Model	Advantages	Disadvantages
Laharz	Very fast. A lahar flow can be prepared in 5 minutes.	Parameters such as erosion depth and rate, solid diameter, which are important parameters in lahars, are not used.
	Easy to enter new lahar flows.	The model is based on filling the valleys and has a geometric progression. It may not reflect realistic results.
	Output sizes are small. File size increases with DEM resolution and the number of DEMs used.	It is highly sensitive to the resolution of DEM.
	Especially in scenario-based studies, it is sufficient to enter only volume and starting points.	Need to use with ArcGIS, and Matlab softwares.
	It is useful for quick research and foresight.	Sometimes ragged edges are seen because of the low DEM quality.
		The starting point is selected manually. Therefore, quite different results can be seen even at very close points.

Model	Advantages	Disadvantages
LaharFlow	The DEM required for modelling is provided automatically by the software.	Although it gives fast results in low volumes (a few hours), it may take days to see the result in high volumes (10^3 m^3 and above) when the simulation time is 5-10 minutes and above.
	It is easy to determine lahar starting points by entering coordinates.	When high volume lahars are entered, the entire file size (including a detailed report and kmz files) can be 100 MB or more.
	Provides a wide range of parameter inputs for better prediction of lahar flows (e.g. erosion depth, granular friction max-min, erosion depth, solid diameter, etc.)	Since the processes take a long time, it is not suitable for obtaining prior knowledge in a short time frame.
	Ragged edges are not observed.	
	It is possible to export data in a very wide range (Table 5).	
	There is no need for any software. It is possible to work online.	

Given all the advantages, disadvantages, and errors arising from the models, the risks that may occur in the Ceniza channel were modelled. Accordingly, hazardous areas are given in Figure 5.3. The cities established along the stream connecting to Ceniza include La Rochela, Ceilan, San Andres Osuna, Panimache and Ingenio-Pantaleon located on the Taniluya barranca, and Las Palmas, part of the Siquinala settlement on the Ceniza barranca, all of which will be at risk.

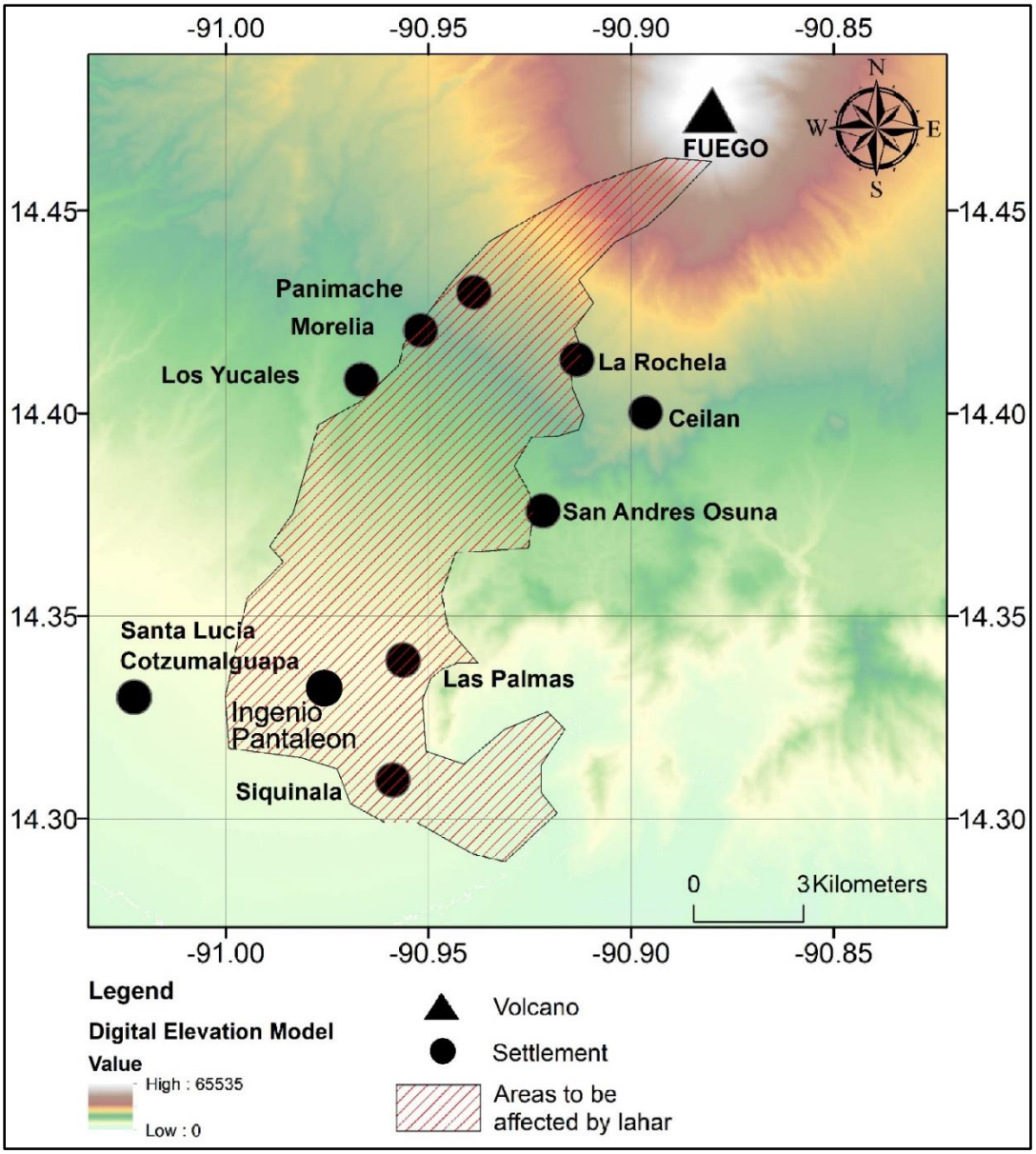

Figure 5.3. The settlements that will be affected by a lahar flow of 10^6 - 10^9 m^3 /s

When both models (Laharz and LaharFlow) are examined, it is seen that Las Palmas is the most vulnerable settlement in the high volume lahar flow that will occur in the Ceniza barranca (Figure 5.1 and Figure 5.2). Laharz modelling demonstrates that this settlement is affected by a lahar flow of 10^7 m^3, while a volume of 10^9 m^3 is required in the LaharFlow model. This is because Laharz is based on a geometric flow, and predicts that the lahar will not overflow from its valley. However, LaharFlow shows that lahar can exit the primary valley, and the flow can merge with other streams.

Siquinala is another settlement that is likely to be inundated. While it was predicted that Siquinala could be inundated in the Laharz modelling, it was predicted that the settlement would

not be inundated in the LaharFlow model. A lahar flow with continuous material flow, eroding, and prolonged duration will be likely to affect the Siqunala.

Ingenio-Pantaleon could be affected by lahars. However, there is an irregularity in the lahar shapes that will affect this area (ragged edges arise in Laharz, Table 6). These irregular shapes are also likely to correlate with DEM quality. It is foreseen that this settlement will not be inundated at LaharFlow. However, since the hazard maps were drawn taking into account the worst conditions, it was concluded that this settlement may also be at risk.

The settlements of La Rochela and San Andres Osuna, located east of Ceniza, will be less at risk than high-risk areas such as Las Palmas and Siquinala. Both models show that these settlements will be affected by a lahar flow of 10^9 m^3.

In both models, among the three settlements located in the west of Ceniza, Panimache, Morelia and Los Yucales, the most fragile settlement is Panimache. A lahar flow of 107 m3 and above will have a devastating effect on this settlement. Morelia and Los Yucales could be affected by lahars of 10^8 m^3 and above.

5.1. Uncertainties

Both models have uncertainties that manifest themselves in areal extent, and real-world decision making much be undertaken with caution. Modelling is conducted by taking into account the physical, topographic, hydrological data, and lahar flows that have previously occurred. For this reason, there are always various uncertainties. For example, in a tropical storm, the amount of precipitation will not be the same all around the volcano. This introduced uncertainty in the lahar volume that can occur.Another difference is the erosion factor. There is erosion up to 5 meters in barranca in Fuego volcano. The effect, solids concentration and destructiveness of lahar, which can occur up to 5 meters with 1 meter of erosion, will be quite different.

Another difference, specific to the LaharFlow model, is the erosion factor. There is erosion up to 20 metres deep in parts of the Ceniza barranca. The effect, solids concentration and destructiveness of lahars, which can occur up to twenty metres with one metre of erosion, will be quite different.

In both models, an exact point must be chosen (assumed) for the lahar's starting point. However, depending on this factor, the direction of the flow and the area it will affect may change.

5.2. Mitigation of risk

There are four methods to minimize lahar risks at Fuego (Figure 5.4). The first of these methods is to avoid hazards. People living in less populated settlements can be shifted to safer areas or can be moved to areas where there is no risk of lahars. This method is a more precise and safe method compared to other methods.

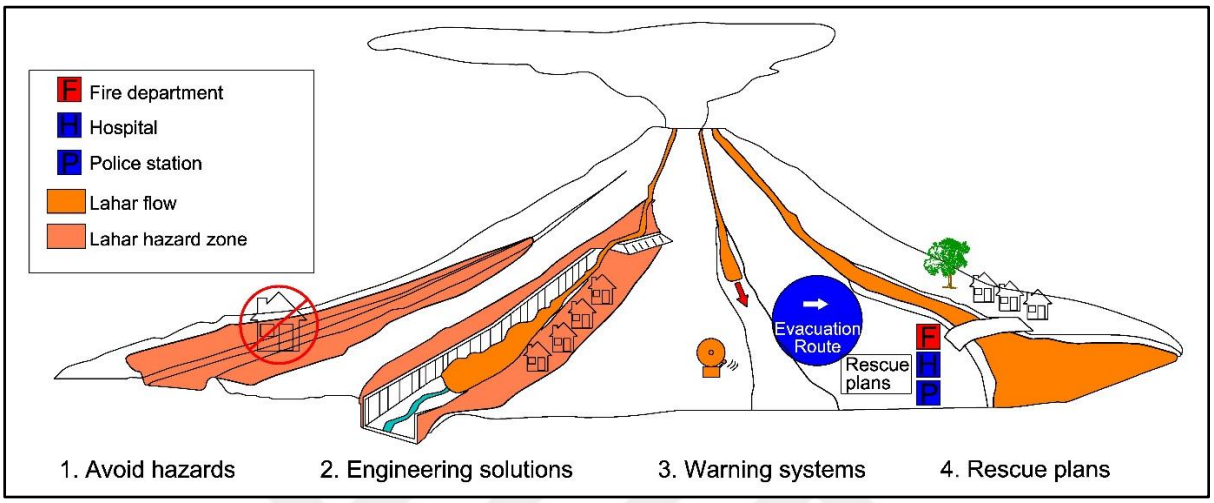

Figure 5.4. Actions to be taken to minimize lahar risks, adapted from Pierson et al., 2014

The second method to reduce risks is to apply engineering solutions in the Ceniza barranca. For this, the base elevation of the Ceniza channel can be lowered. Although this method is a costly and time-consuming solution, the Las Palmas, Siquinala and Ingenio-Pantaleon settlements, which may be affected by the overflow of the bed, can be protected in the long term.

The third solution is to place early warning systems for lahar hazards. In this method, sensors are placed to detect when the lahar flow starts. Data from the hazard area and precipitation data are evaluated by experts. Accordingly, it is decided whether there is a lahar threat or not.

The fourth solution is to prepare for rescue plans. In other words, if a lahar occurs, people should be evacuated safely. Appropriate plans for this are given in Table 4. In addition, signs that people can easily follow should be placed for a safe evacuation. In this way, people can be prevented from acting in panic during a disaster.

Local administrators, policymakers and volcanologists should also work in harmony for the safe and most reasonable implementation of all these methods.

6. Conclusions

Fuego is a very active volcano, and frequent lahars cause loss of life and property. As a result of the activities of the volcano throughout history, pyroclastic materials ($5.24x10^7$ m^3 (between 1999-2012) + $3.00x10^7$ m^3 (2018 Eruption)= 8.24×10^7 m^3) have accumulated around the volcano.

As a result of the combination of this material with water (in a tropical storm condition), there may be severe lahar flows in the Ceniza barranca. The triggering (the amount of precipitation required for a lahar to start) of these lahars will be approximately 10.00 mm. However, in topical storms, this amount of rainfall can reach 287.20 mm and above. This indicates that a lahar flow of up to 10^8 m^3 can occur. To identify the areas that will be affected by lahar flows, lower volumes (10^6 and 10^7 m3) were modelled. Besides, the worst-case scenario conditions (10^9 m^3) that could occur were also examined.

In this evaluation, the previous eruptions and their potentials were also examined. Differences were observed in Laharz and LaharFlow programs used in the modelling. The reasons for these differences include (1) the parameters used by the programs, and (2) their working principles. Also, their advantages/disadvantages have been analysed in detail.

Currents that may occur as a result of a tropical storm in the Ceniza barranca will advance in three branches. The first is the flow that will take place over the Ceniza barranca. In such a flow, the Siquinala, Las Palmas and Ingenio-Pantaleon settlements will be at risk.

The second is the lahar flow that will advance in the Taniluya barranca if the lahar flow exceeds the capacity of the Ceniza barranca. This flow would cause damage to the Panimache and Morelia settlements, while damage is likely to be more limited in the Los Yucales settlement.

The third is the flow that will occur in the Platanares and Melina rivers, which are connected to the Ceniza River. It is expected that La Rochela and San Andres Osuna settlements will be affected by this flow.

It is possible to minimize and eliminate risks using the following methods. (1) Moving settlements with a low population density is a solution to reduce the risks. (2) Use the evacuation routes far away from the source of the volcano and the Ceniza barranca. (3) With engineering solutions, lahars can be prevented from exiting the valley (lowering the elevation of the valley floor using dredging) or through the use of flood defences. Stakeholders implementing these methods need to work in partnership with volcanologists and managers in Guatemala.

7. References

Álvarez-Gómez, J. A., Meijer, P. T., Martínez-Díaz, J. J., & Capote, R. (2008). Constraints from finite element modeling on the active tectonics of northern Central America and the Middle America Trench. Tectonics, 27(1). https://doi.org/10.1029/2007TC002162

Auker, M. R., Sparks, R. S. J., Siebert, L., Crosweller, H. S., & Ewert, J. (2013). A statistical analysis of the global historical volcanic fatalities record. Journal of Applied Volcanology, 2(1), 2. https://doi.org/10.1186/2191-5040-2-2

Authemayou, C., Brocard, G., Teyssier, C., Simon-Labric, T., Guttiérrez, A., Chiquín, E. N., & Morán, S. (2011). The Caribbean–North America–Cocos Triple Junction and the dynamics of the Polochic–Motagua fault systems: Pull-up and zipper models. Tectonics, 30(3). https://doi.org/10.1029/2010TC002814

Blackburn, E. A., Wilson, L., & Sparks, R. J. (1976). Mechanisms and dynamics of strombolian activity. Journal of the Geological Society, 132(4), 429-440. https://doi.org/10.1144/gsjgs.132.4.0429

Bonis, S. (1993). Mapa Geologico General de Guatemala, 1:250.000, Guatemala, Instituto Geografico Militar. https://volcano.si.edu/volcano.cfm?vn=342090, Accessed date: 03 July 2020.

Cando-Jácome, M., & Martínez-Graña, A. (2019). Determination of Primary and Secondary Lahar Flow Paths of the Fuego Volcano (Guatemala) Using Morphometric Parameters. Remote Sensing, 11(6), 727. https://doi.org/10.3390/rs11060727

Canuti, P., Casagli, N., Catani, F., & Falorni, G. (2002). Modelling of the Guagua Pichincha volcano (Ecuador) lahars. Physics and Chemistry of the Earth, Parts A/B/C, 27(36), 1587-1599. https://doi.org/10.1016/S1474-7065(02)00180-8

Chesner, C. A., & Rose Jr, W. I. (1984). Geochemistry and evolution of the Fuego volcanic complex, Guatemala. Journal of Volcanology and Geothermal Research, 21(1-2), 25-44. https://doi.org/10.1016/0377-0273(84)90014-3

Duffield, W. A., Heiken, G. H., Wohletz, K. H., Maassen, L. W., Dengo, G., McKee, E. H., & Castañeda, O. (1992). Geology and geothermal potential of the Tecuamburro volcano area, Guatemala. Geothermics, 21(4), 425-446. https://doi.org/10.1016/0375-6505(92)90001-P

Earthexplorer, USGS. [online] Available at: <https://earthexplorer.usgs.gov/> [Accessed 29 August 2020].

Escobar-Wolf, R., 2013. Volcanic Processes and Human Exposure as Elements to Build a Risk Model for Volcan de Fuego, Guatemala. (PhD thesis). Retrieved from:. https://digitalcommons.mtu.edu/etds/638, Accessed date: 26 June 2020.

Global Volcanism Program, 2009. Report on Fuego (Guatemala) (Wunderman, R., ed.). Bulletin of the Global Volcanism Network, 34:12. Smithsonian Institution. https://doi.org/10.5479/si.GVP.BGVN200912-342090.

Global Volcanism Program, 2011. Report on Fuego (Guatemala) (Herrick, J.A., and Wunderman, R., eds.). Bulletin of the Global Volcanism Network, 36:6. Smithsonian Institution. https://doi.org/10.5479/si.GVP.BGVN201106-342090.

Global Volcanism Program, 2013. Report on Fuego (Guatemala) (Herrick, J.A., and Wunderman, R., eds.). Bulletin of the Global Volcanism Network, 38:5. Smithsonian Institution. https://doi.org/10.5479/si.GVP.BGVN201305-342090.

Global Volcanism Program, 2013. [Fuego (342090)] in Volcanoes of the World, v. 4.9.0 (04 Jun 2020). Venzke, E (ed.). Smithsonian Institution. Downloaded 20 Jun 2020 ([https://volcano.si.edu/volcano.cfm?vn=342090]).

Global Volcanism Program, 2014. Report on Fuego (Guatemala) (Herrick, J.A., and Wunderman, R., eds.). Bulletin of the Global Volcanism Network, 39:4. Smithsonian Institution. https://doi.org/10.5479/si.GVP.BGVN201404-342090.

Global Volcanism Program, 2017. Report on Fuego (Guatemala) (Crafford, A.E., and Venzke, E., eds.). Bulletin of the Global Volcanism Network, 42:5. Smithsonian Institution. https://doi.org/10.5479/si.GVP.BGVN201705-342090.

Global Volcanism Program, 2017. Report on Fuego (Guatemala) (Crafford, A.E., and Venzke, E., eds.). Bulletin of the Global Volcanism Network, 42:11. Smithsonian Institution. https://doi.org/10.5479/si.GVP.BGVN201711-342090.

Global Volcanism Program, 2018. Report on Fuego (Guatemala) (Crafford, A.E., and Venzke, E., eds.). Bulletin of the Global Volcanism Network, 43:2. Smithsonian Institution. https://doi.org/10.5479/si.GVP.BGVN201802-342090.

Global Volcanism Program, 2018. Report on Fuego (Guatemala) (Crafford, A.E., and Venzke, E., eds.). Bulletin of the Global Volcanism Network, 43:8. Smithsonian Institution. https://doi.org/10.5479/si.GVP.BGVN201808-342090.

Global Volcanism Program, 2019. Report on Fuego (Guatemala) (Krippner, J.B., and Venzke, E., eds.). Bulletin of the Global Volcanism Network, 44:4. Smithsonian Institution. https://doi.org/10.5479/si.GVP.BGVN201904-342090.

Global Volcanism Program, 2019. Report on Fuego (Guatemala) (Crafford, A.E., and Venzke, E., eds.). Bulletin of the Global Volcanism Network, 44:10. Smithsonian Institution. https://doi.org/10.5479/si.GVP.BGVN201910-342090.

Google Earth Pro 7.3.3.7699, (27 June, 2020). Volcán de Fuego, Guatemala. Lat 14.373657°, Lon -90.893915°, eye alt 39.14 km, http://www.earth.google.com

"Guatemala: Estimaciones De La Población Total Por Municipio. Período 2008-2020. (Al 30 De Junio)." Instituto Nacional De Estadistica, www.oj.gob.gt/estadisticaj/reportes/poblacion-total-por-municipio(1).pdf. Accessed Date: 16 July 2020

ICC, Private Institute for Climate Change Research, 2019. https://redmet.icc.org.gt/ Accessed Date: 03 July 2020.

Iverson, R. M., Schilling, S. P., & Vallance, J. W. (1998). Objective delineation of lahar-inundation hazard zones. Geological Society of America Bulletin, 110(8), 972-984. https://doi.org/10.1130/0016-7606(1998)110<0972:ODOLIH>2.3.CO;2

Iverson, R. M. (2003). "How should mathematical models of geomorphic processes be judged?" in Prediction in Geomorphology, Vol. 135, eds P. R. Wilcock and R. M. Iverson (Washington, DC: Geophysical Monograph Series, American Geophysical Union), 83–94. http://mechanism.ucsd.edu/~bill/ModelsAndPrediction/papers/2003.IversonPrediction.AGUbook.2003.pdf. Accessed Date: 31 August 2020.

Jones, R., Manville, V., Peakall, J., Froude, M. J., & Odbert, H. M. (2017). Real-time prediction of rain-triggered lahars: incorporating seasonality and catchment recovery. Natural Hazards and Earth System Science, 17(12), 2301-2312. https://doi.org/10.5194/nhess-17-2301-2017

Kantha, L. (2006). Time to replace the Saffir-Simpson hurricane scale?. Eos, Transactions American Geophysical Union, 87(1), 3-6. https://doi.org/10.1029/2006EO010003

Kurtz, A.W., 1913. Documentos Antiguos: Copia de dos cartas manuscritas de Don Pedro de Alvarado a Hernando Cortes, 11 de abril y 28 de julio 1524.

Lyons, J. J., Waite, G. P., Rose, W. I., & Chigna, G. (2010). Patterns in open vent, strombolian behaviour at Fuego volcano, Guatemala, 2005–2007. Bulletin of volcanology, 72(1), 1. https://doi.org/10.1007/s00445-009-0305-7

Martin, D. P., & Rose Jr, W. I. (1981). Behavioural patterns of Fuego volcano, Guatemala. Journal of Volcanology and Geothermal Research, 10(1-3), 67-81. https://doi.org/10.1016/0377-0273(81)90055-X

Naismith, A. K., Watson, I. M., Escobar-Wolf, R., Chigna, G., Thomas, H., Coppola, D., & Chun, C. (2019). Eruption frequency patterns through time for the current (1999–2018) activity cycle at Volcán de Fuego derived from remote sensing data: Evidence for an accelerating cycle of explosive paroxysms and potential implications of eruptive activity. Journal of Volcanology and Geothermal Research, 371, 206-219. https://doi.org/10.1016/j.jvolgeores.2019.01.001

Ogburn, S. E., & Calder, E. S. (2017). The relative effectiveness of empirical and physical models for simulating the dense undercurrent of pyroclastic flows under different emplacement conditions. Frontiers in Earth Science, 5, 83. DOI: 10.3389/feart.2017.00083

Pardini, F., Queißer, M., Naismith, A., Watson, I. M., Clarisse, L., & Burton, M. R. (2019). Initial constraints on triggering mechanisms of the eruption of Fuego volcano (Guatemala) from 3 June 2018 using IASI satellite data. Journal of Volcanology and Geothermal Research, 376, 54-61. https://doi.org/10.1016/j.jvolgeores.2019.03.014

Patrick, M. R., Harris, A. J., Ripepe, M., Dehn, J., Rothery, D. A., & Calvari, S. (2007). Strombolian explosive styles and source conditions: insights from thermal (FLIR) video. Bulletin of volcanology, 69(7), 769-784. https://doi.org/10.1007/s00445-006-0107-0

Pierson, T. C., Wood, N. J., & Driedger, C. L. (2014). Reducing risk from lahar hazards: concepts, case studies, and roles for scientists. Journal of Applied Volcanology, 3(1), 16. https://doi.org/10.1186/s13617-014-0016-4

Rader, E., Geist, D., Geissman, J., Dufek, J., Harpp, K., 2015. Hot class and cold blasts: thermal heterogeneity in boiling-over pyroclastic density currents. Geol. Soc. Lond., Spec. Publ. 396 (1), 67–86. https://doi.org/10.1144/SP396.16

Rodolfo, K. S. (1989). Origin and early evolution of lahar channel at Mabinit, Mayon Volcano, Philippines. Geological Society of America Bulletin, 101(3), 414-426. https://doi.org/10.1130/0016-7606(1989)101<0414:OAEEOL>2.3.CO;2

Roggensack, K. (2001). Unravelling the 1974 eruption of Fuego volcano (Guatemala) with small crystals and their young melt inclusions. Geology, 29(10), 911-914. https://doi.org/10.1130/0091-7613(2001)029<0911:UTEOFV>2.0.CO;2

Smith, G. A., & Fritz, W. J. (1989). Volcanic influences on terrestrial sedimentation. Geology, 17(4), 375-376. https://doi.org/10.1130/0091-7613(1989)017<0375:VIOTS>2.3.CO;2

Sparks, R. S. J., and Aspinall, W. P. (2004). "Volcanic activity: frontiers and challenges in forecasting, prediction and risk assessment," in The State of the Planet: Frontiers and Challenges in Geophysics, eds R. S. J. Sparks and C. J. Hawkesworth (Washington, DC: American Geophysical Union). DOI: 10.1029/150GM28

US Department of Commerce, National Oceanic and Atmospheric Administration. Tropical Cyclone Climatology, www.nhc.noaa.gov/climo/#:~:text=Atlantic%20%26%20Eastern%20Pacific%20Climatology, extends%20to%20140°W. Accessed date: 05 July 2020

US Department of Commerce, National Oceanic and Atmospheric Administration. "What Is a Hurricane?" NOAA's National Ocean Service, 28 June 2013, https://www.oceanservice.noaa.gov/facts/hurricane.html#:~:text=A%20hurricane%20is%20a%20type,over%20tropical%20or%20subtropical%20waters.&text=When%20a%20storm's%20maximum%20sustained,a%20hurricane's%20maximum%20sustained%20winds. Accessed date: 05 July 2020

Vallance, J. W., & Iverson, R. M. (2015). Chapter 37 - Lahars and Their Deposits, Editor(s): Haraldur Sigurdsson, The Encyclopedia of Volcanoes (Second Edition), Academic Press, 2015, Pages 649-664, ISBN 9780123859389, https://doi.org/10.1016/B978-0-12-385938-9.00037-7.

Vargas Franco, R. D., Thouret, J. C., Delaite, G., Van Westen, C. J., Sheridan, M. F., Siebe C., Mariño, J., Souriot, T., Stinton, A. (2010). Mapping and assessing volcanic and flood hazards and risks, with emphasis on lahars, in Arequipa, Peru. Stratigraphy and Geology of Volcanic Areas. GSA Special Papers, v. 464, 2010. DOI: 10.1130/2010.2464(13)

Webley, P.W., Wooster, M.J., Strauch, W., Saballos, J.A., Dill, K., Stephenson, P., Stephenson, J., Escobar Wolf, R., Matias, O., 2008. Experiences from near-real-time satellite-based volcano monitoring in Central America: case studies at Fuego, Guatemala. Int. J. Remote Sens. 29 (22), 6621–6646. https://doi.org/10.1080/01431160802168301.

Woodhouse, M., Hogg, A., Phillips, J. (2016), LaharFlow (2016). Retrieved September 02, 2020, from https://www.laharflow.bris.ac.uk/

8. Appendices

Modeling in LaharFlow (10^6 m^3)

LaharFlow

Model parameters

Domain settings

Latitude:	14.47	*x resolution:*	30.00 m
Longitude:	-90.88	*y resolution:*	30.00 m
Domain size in x:	40000 m	*Simulation time:*	3600 s
Domain size in y:	40000 m		

Source settings

No cap sources

Flux source 1

Latitude:	14.45			
Longitude:	-90.90			
x position:	–			
y position:	–			
Radius:	50.00 m			
Time series:	time (s)	0	250.0	2500
	flux (m^3/s)	0	800.0	0
	concentration	0.2000	0.2000	0.2000

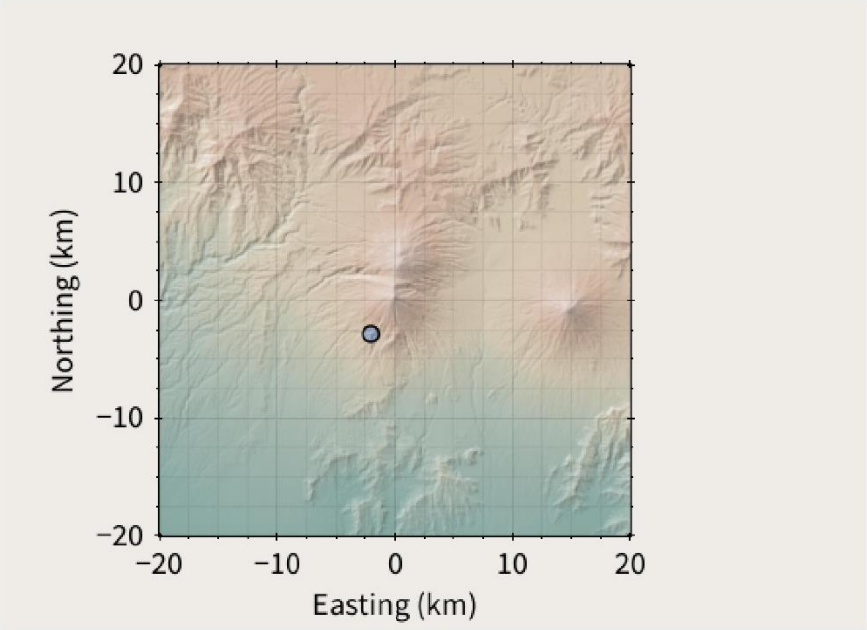

Parameters

Ch'ezy coefficient:	0.04000	*Erosion rate:*	0.001000
Granular friction minimum slope:	0.1000	*Erosion depth:*	4.000 m
Granular friction maximum slope:	0.4000	*Bed porosity:*	0.3500
Friction switch value:	0.2000	*Solid diameter:*	0.01000 m
Friction switch rate:	3.000		

Report generated by LaharFlow, URL https://www.laharflow.bristol.ac.uk Generated at 14:33 2020-07-13

Topography

Using 30m SRTM topography

Model results

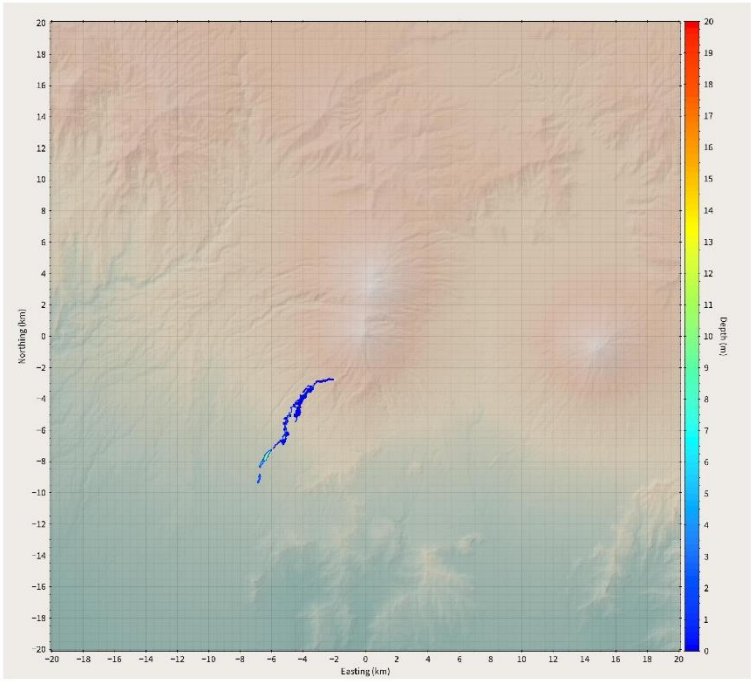

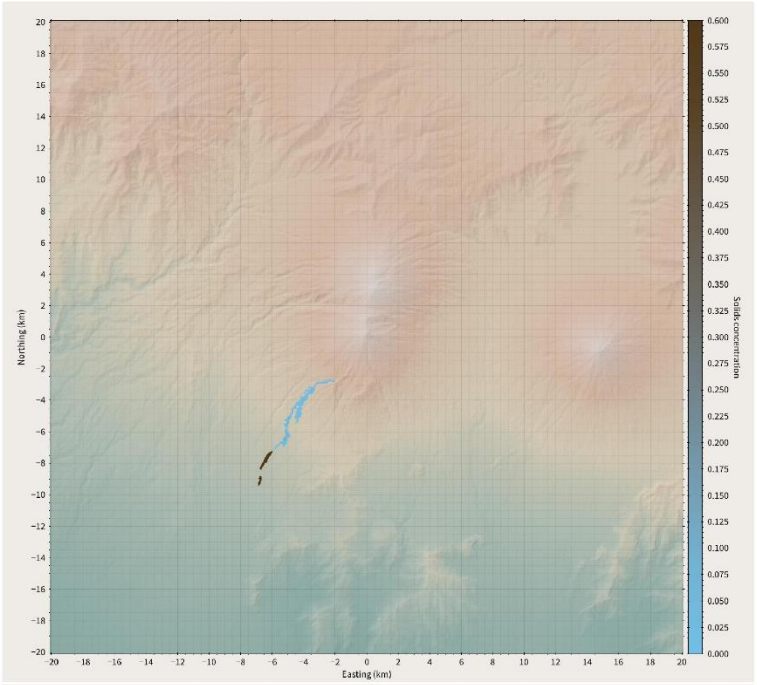
Northing (km)
Easting (km)
Solids concentration

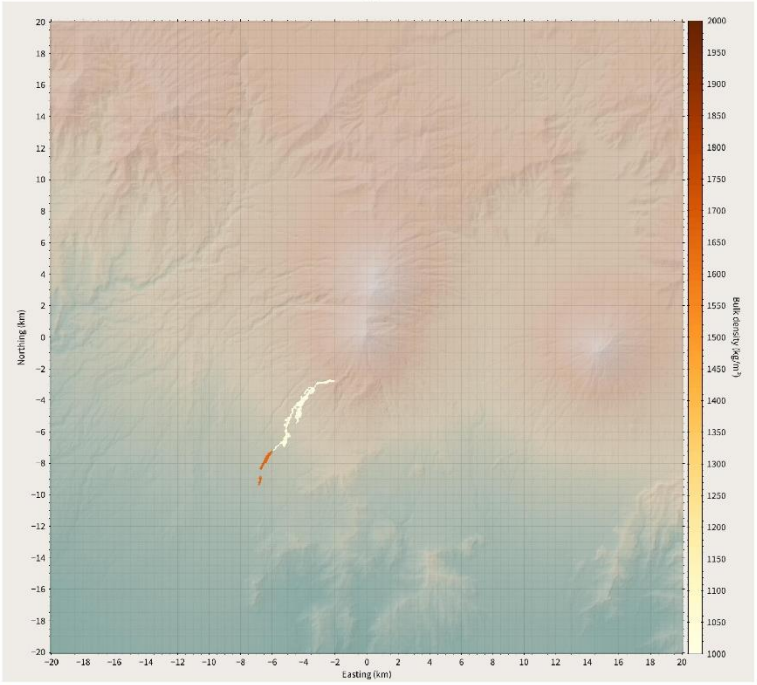
Northing (km)
Easting (km)
Bulk density (kg/m³)

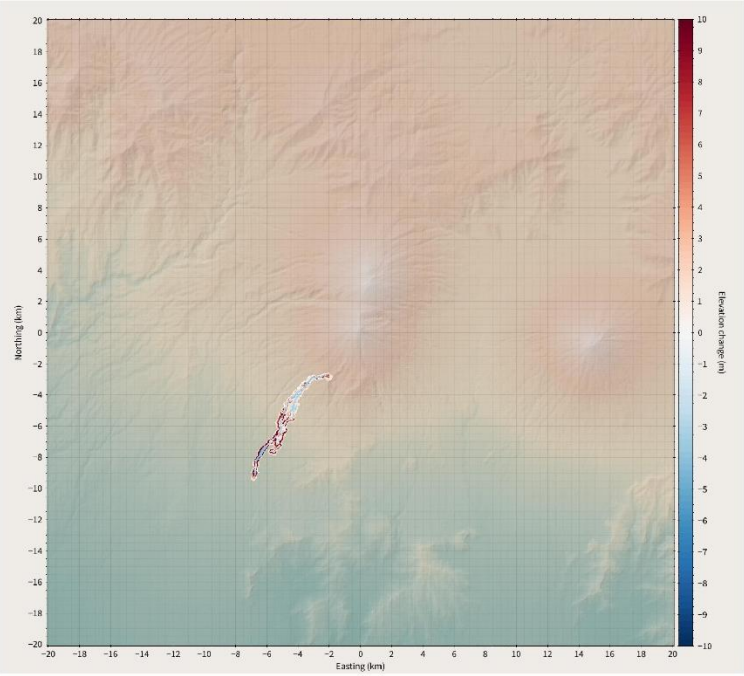
Northing (km)
Easting (km)
Elevation change (m)

Modeling in LaharFlow (10^7 m^3)

Model parameters

Domain settings

Latitude:	14.47	*x resolution:*	30.00 m
Longitude:	-90.88	*y resolution:*	30.00 m
Domain size in x:	40000 m	*Simulation time:*	3600 s
Domain size in y:	40000 m		

Source settings

No cap sources

Flux source 1

Latitude:	14.45			
Longitude:	-90.89			
x position:	–			
y position:	–			
Radius:	50.00 m			
Time series:	time (s)	0	250.0	2500
	flux (m^3/s)	0	8000	0
	concentration	0.2000	0.2000	0.2000

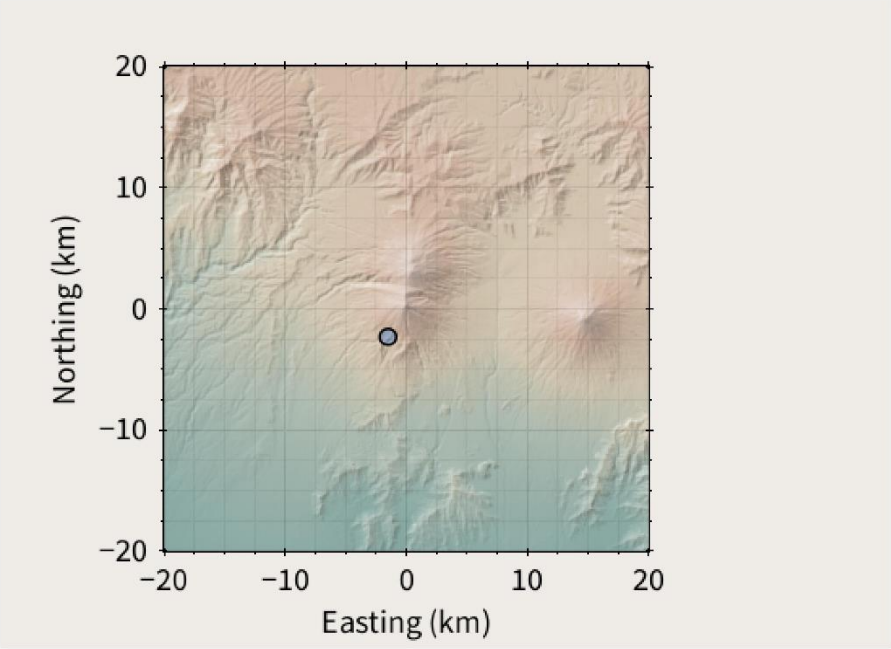

Parameters

Ch'ezy coefficient:	0.04000	*Erosion rate:*	0.001000
Granular friction minimum slope:	0.1000	*Erosion depth:*	4.000 m
Granular friction maximum slope:	0.4000	*Bed porosity:*	0.3500
Friction switch value:	0.2000	*Solid diameter:*	0.01000 m
Friction switch rate:	3.000		

Topography

Using 30m SRTM topography

Model results

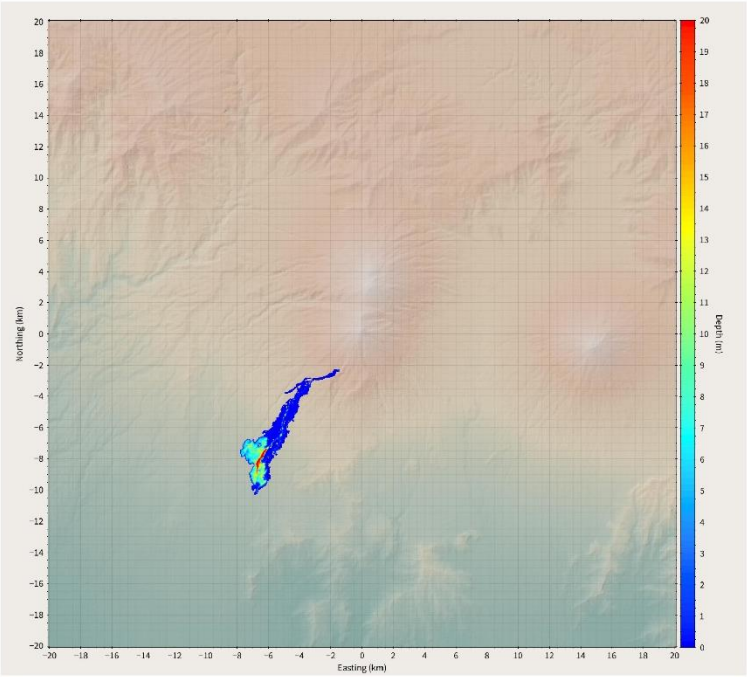

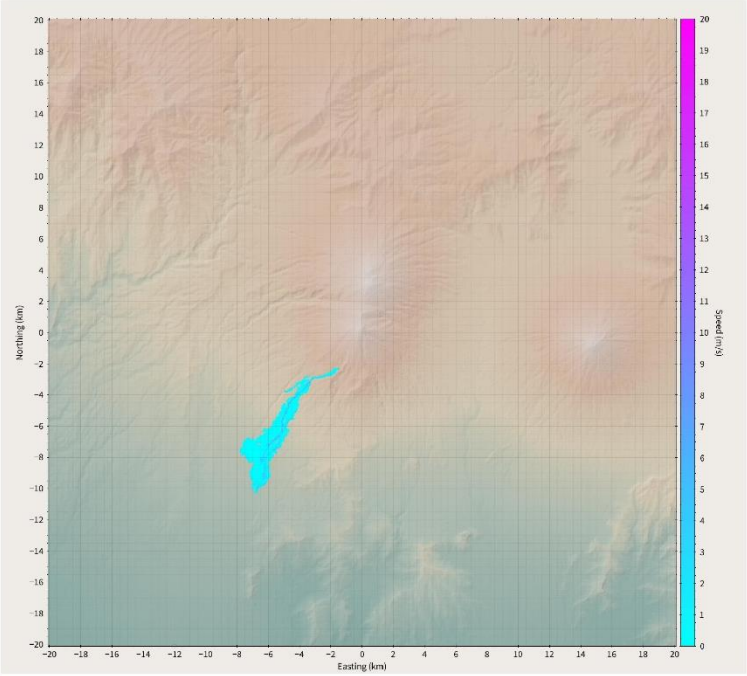

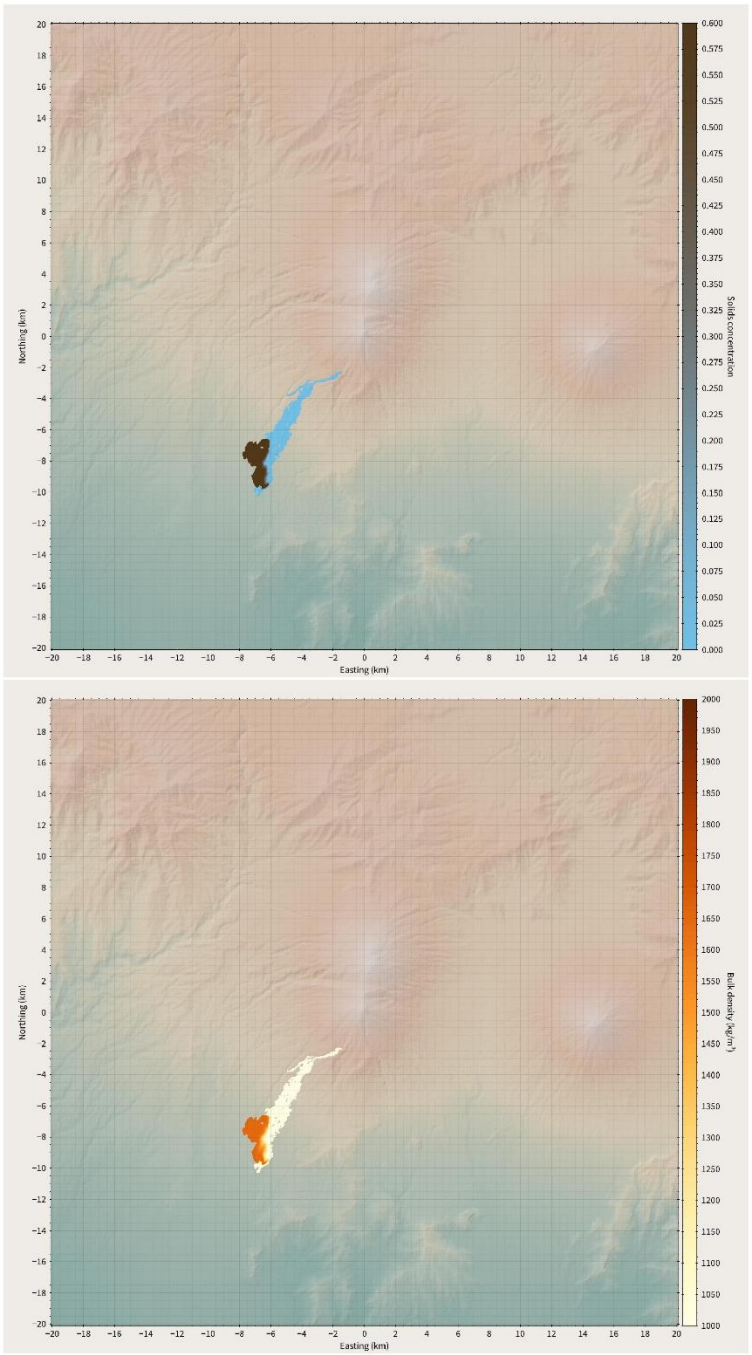
Northing (km)
Easting (km)
Solids concentration
Bulk density (kg/m³)

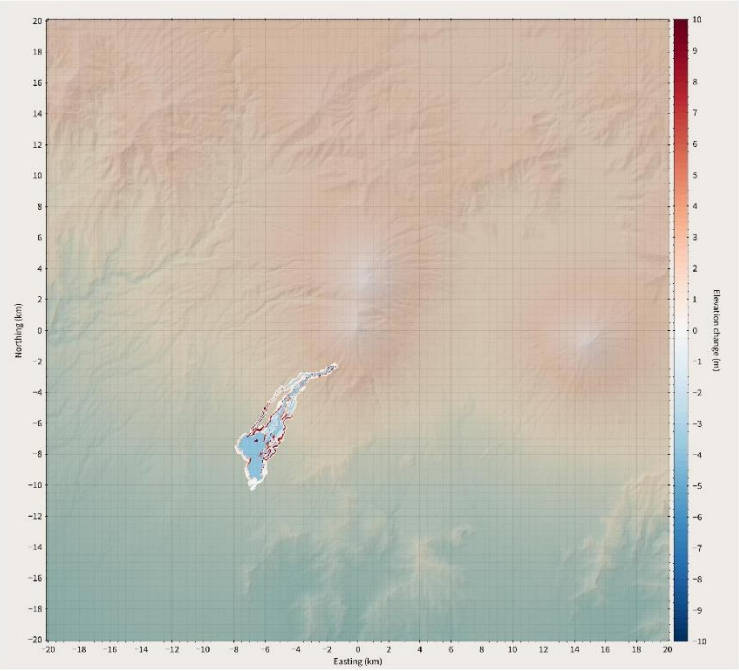
Northing (km)
Easting (km)
Elevation change (m)

Modeling in LaharFlow (10^8 m^3)

LaharFlow

Model parameters

Domain settings

Latitude:	14.47	*x resolution:*	30.00 m
Longitude:	-90.88	*y resolution:*	30.00 m
Domain size in x:	40000 m	*Simulation time:*	3600 s
Domain size in y:	40000 m		

Source settings

No cap sources

Flux source 1

Latitude:		14.45		
Longitude:		-90.90		
x position:		–		
y position:		–		
Radius:		50.00 m		
Time series:	time (s)	0	250.0	2500
	flux (m^3/s)	0	80000	0
	concentration	0.2000	0.2000	0.2000

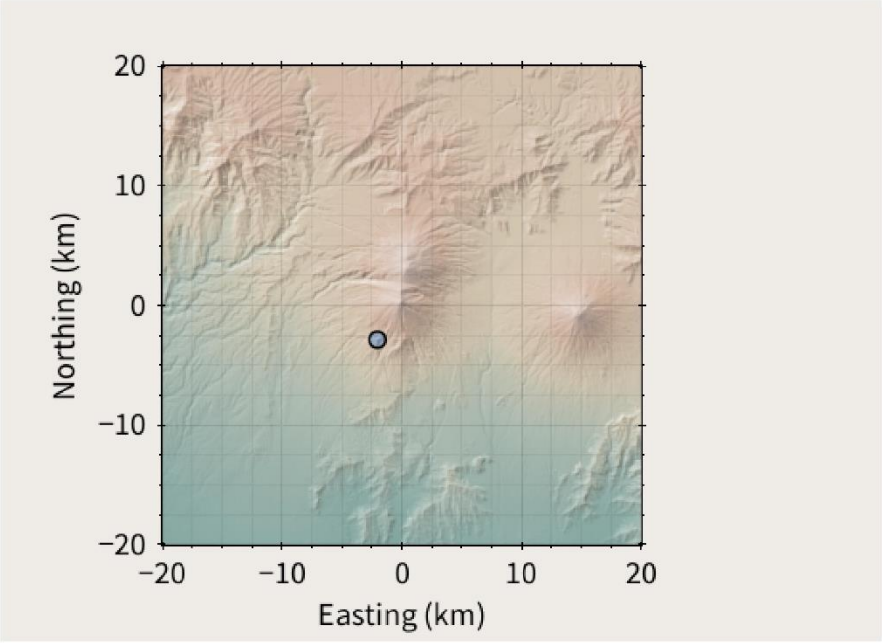

Parameters

Ch'ezy coefficient:	0.04000	*Erosion rate:*	0.001000
Granular friction minimum slope:	0.1000	*Erosion depth:*	4.000 m
Granular friction maximum slope:	0.4000	*Bed porosity:*	0.3500
Friction switch value:	0.2000	*Solid diameter:*	0.01000 m
Friction switch rate:	3.000		

Topography

Using 30m SRTM topography

Model results

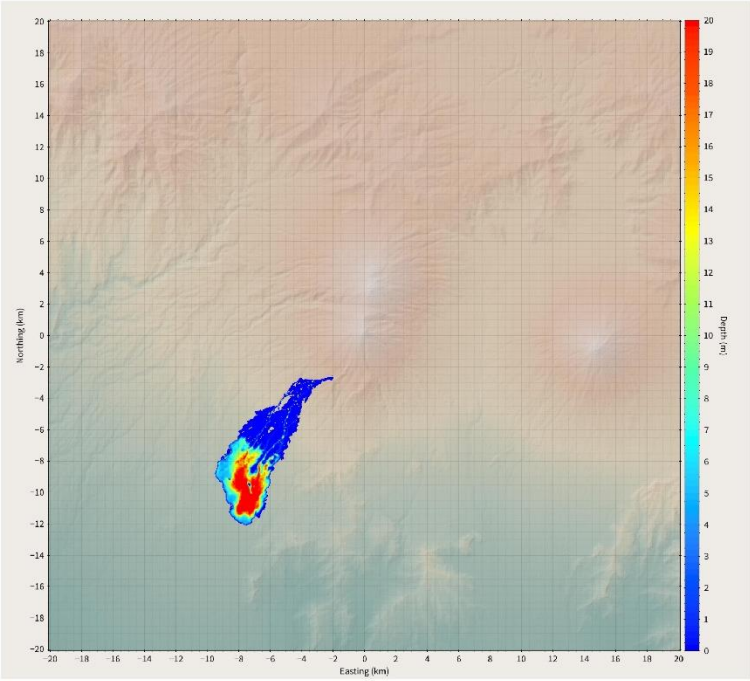

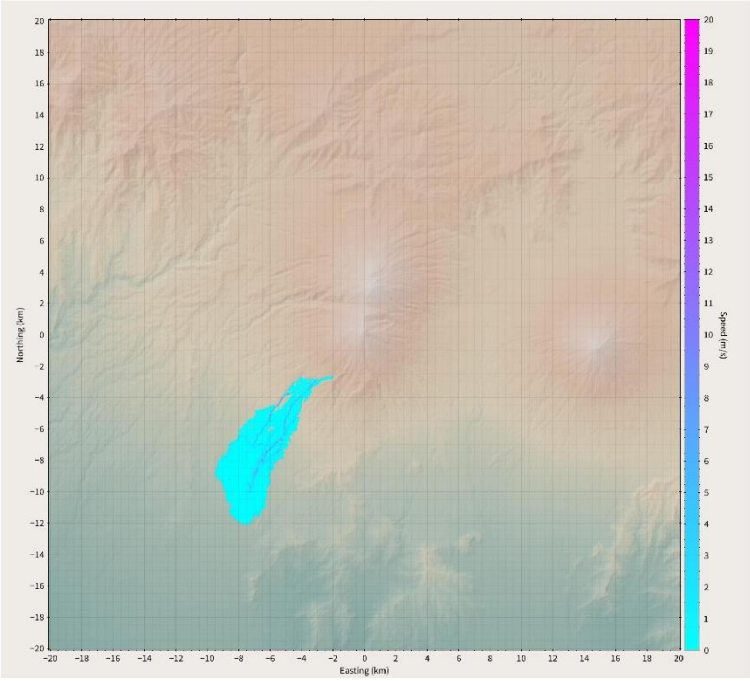

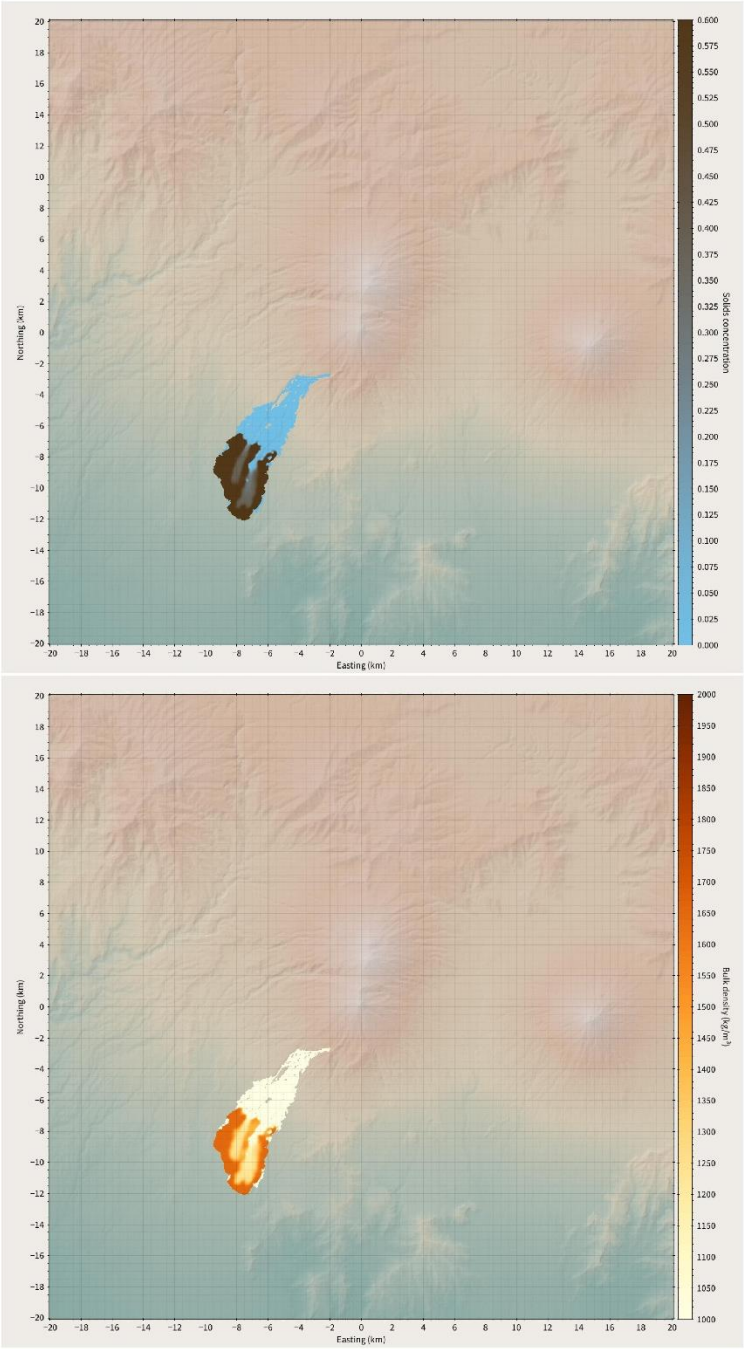
Northing (km)
Easting (km)
Solids concentration
Bulk density (kg/m³)

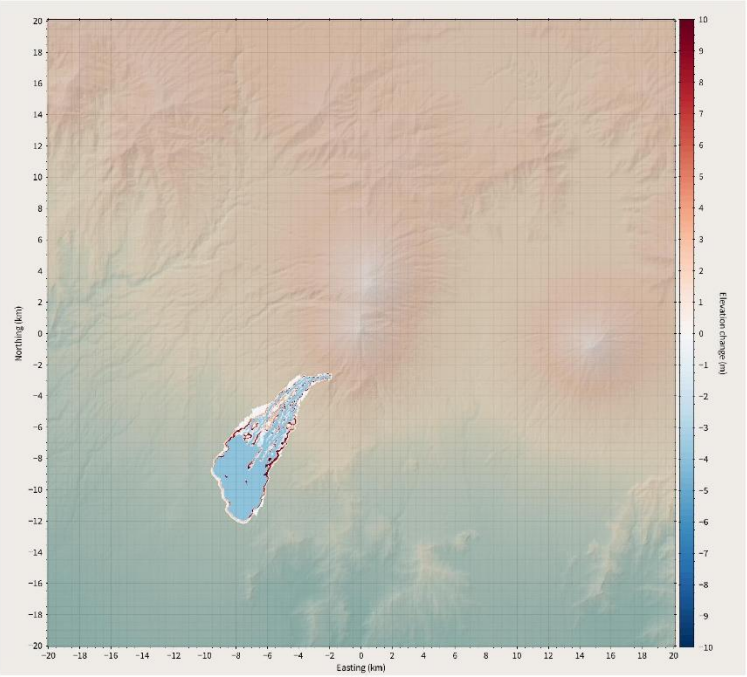
Northing (km)
Easting (km)
Elevation change (m)

Modeling in LaharFlow (10^9 m^3)

Model parameters

Domain settings

Latitude:	14.47	*x resolution:*	30.00 m
Longitude:	-90.88	*y resolution:*	30.00 m
Domain size in x:	40000 m	*Simulation time:*	3600 s
Domain size in y:	40000 m		

Source settings

No cap sources

Flux source 1

Latitude:		14.45		
Longitude:		-90.90		
x position:		–		
y position:		–		
Radius:		50.00 m		
Time series:	time (s)	0	250.0	2500
	flux (m^3/s)	0	8.000×10^5	0
	concentration	0.2000	0.2000	0.2000

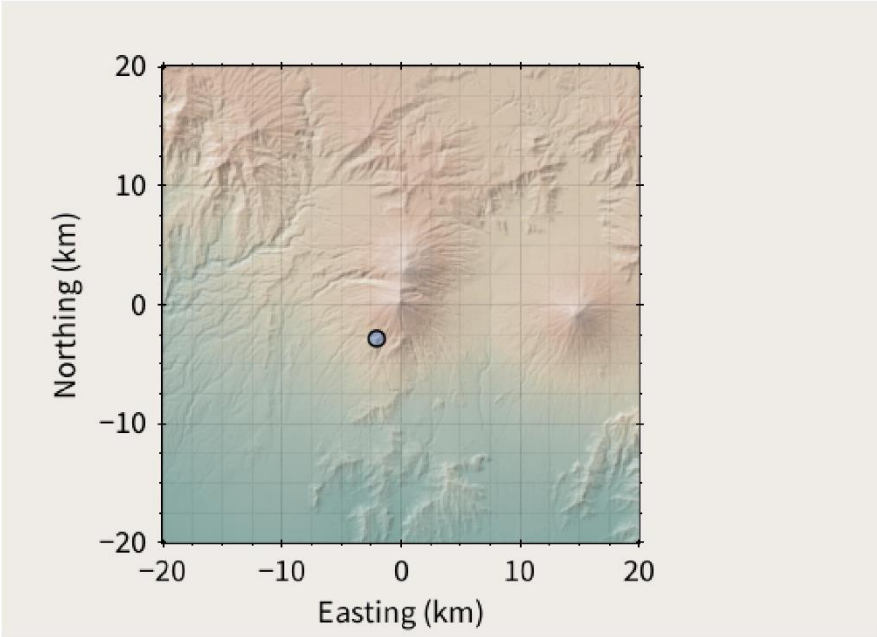

Parameters

Ch'ezy coefficient:	0.04000	*Erosion rate:*	0.001000
Granular friction minimum slope:	0.1000	*Erosion depth:*	4.000 m
Granular friction maximum slope:	0.4000	*Bed porosity:*	0.3500
Friction switch value:	0.2000	*Solid diameter:*	0.01000 m
Friction switch rate:	3.000		

Topography

Using 30m SRTM topography

Model results

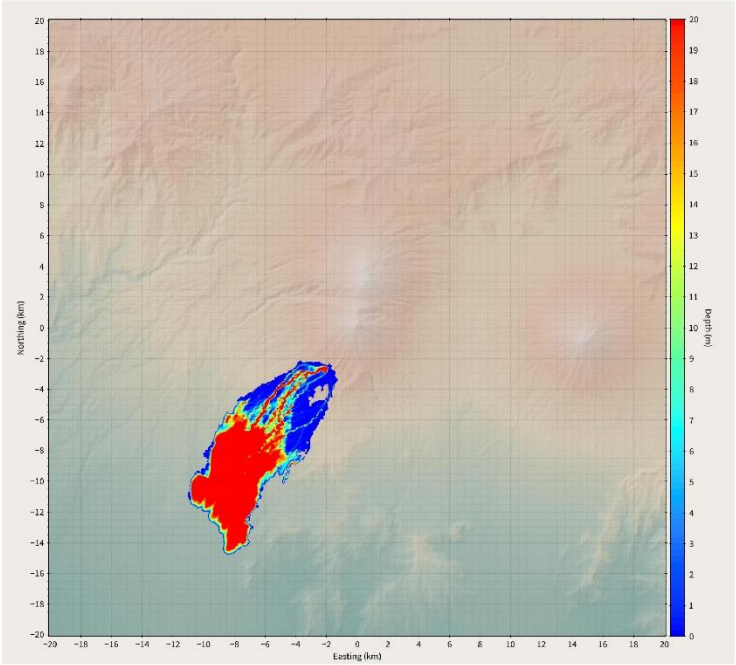

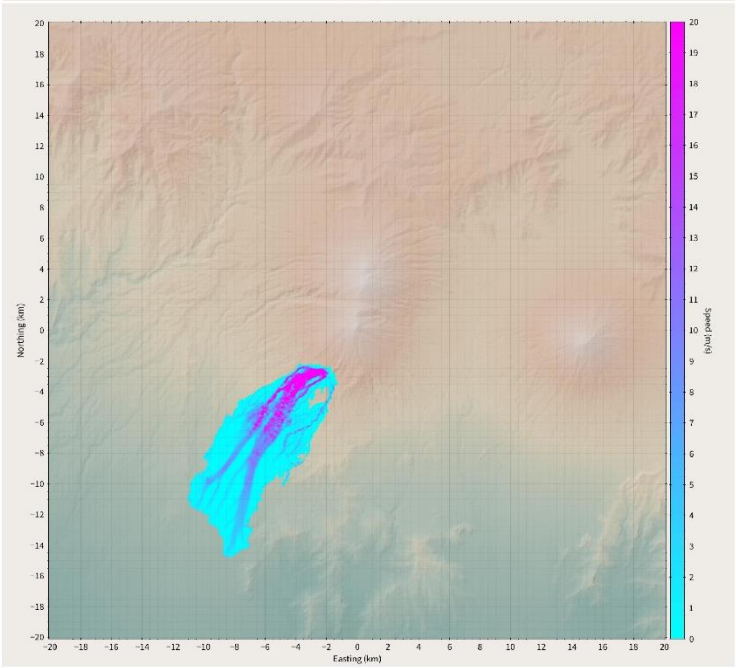

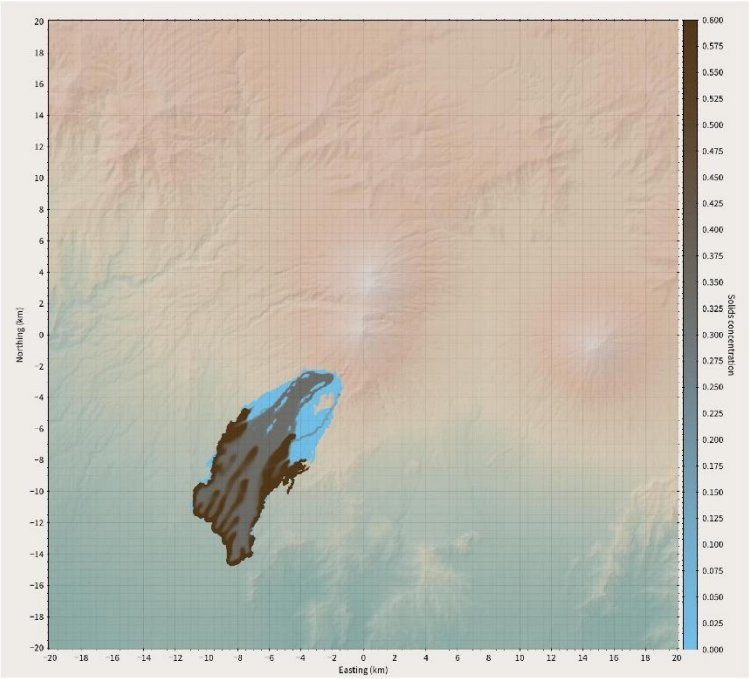
Northing (km)
Easting (km)
Solids concentration

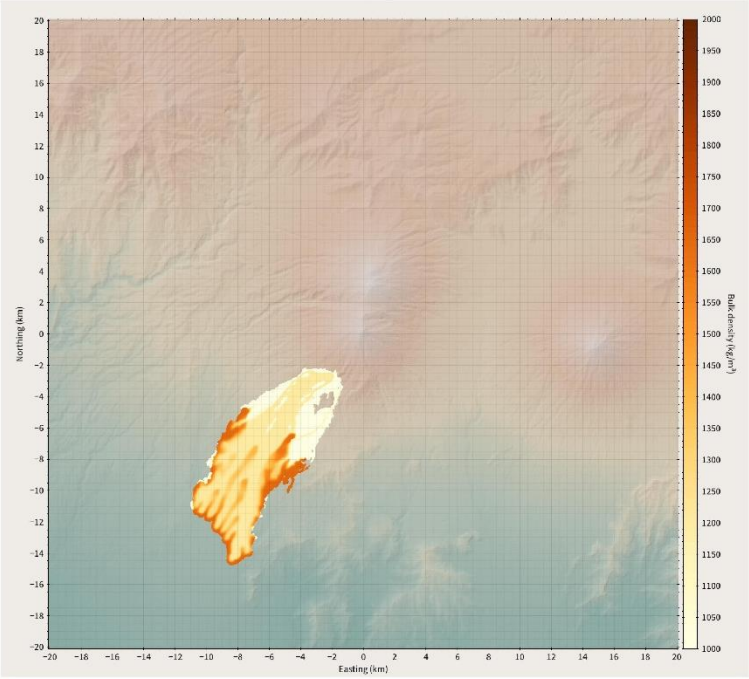
Northing (km)
Easting (km)
Bulk density (kg/m³)

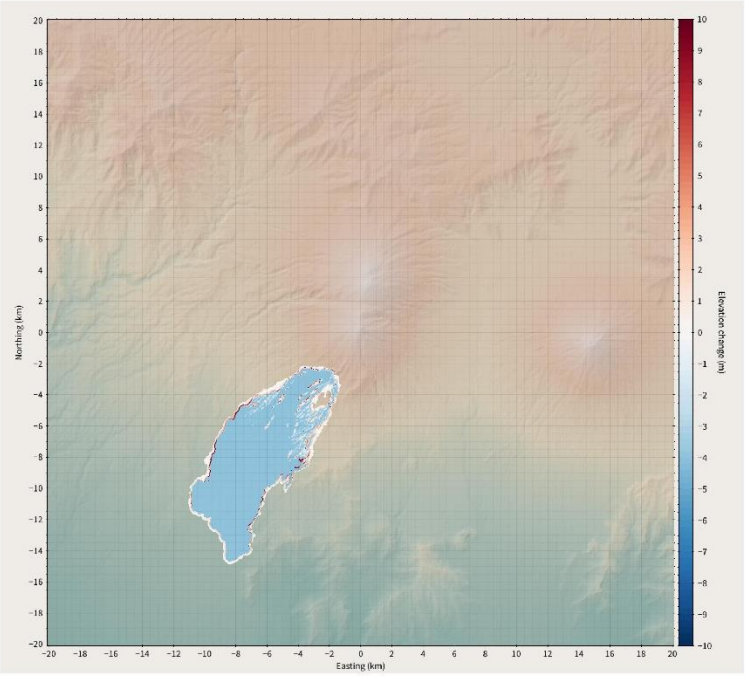
Northing (km)
Easting (km)
Elevation change (m)